GERMAN-MONGOLIAN INSTITUTE FOR RESOURCES AND TECHNOLOGY

The present work was submitted to the Faculty of Mechanical and Electrical Engineering

SAG MILL - Design improvement for prevention form water leakage

Bachelor Thesis

by
Naranmisheel Baljinnyam

Supervisor 1 ***Prof. Dr. Odbileg Norovrinchen***
Supervisor 2 ***Mr. Gurragchaa Tumur***

Ulaanbaatar/Nalaikh, 1/2/2026

Acknowledgement

I want to express my heartfelt gratitude to everyone who supported me throughout this thesis.

First and foremost, my deepest appreciation goes to my first supervisor, PhD. Odbileg, for his guidance, encouragement, and support throughout my student years. I am also grateful to Mr.Gurragchaa, my second supervisor, for his dedicated supervision and expert advice on this thesis.

I am grateful to Dorjsuren from Oyu Tolgoi LLC for his expertise and guidance in data acquisition and his support through my internship and making the field measurements possible.

Finally, I thank my family, friends, and everyone who helped along the way for their patience and kindness.

Abstract

Semi-autogenous grinding (SAG) mills at the Oyu Tolgoi copper-gold concentrator in Mongolia are the primary comminution assets of the operation, each rated at 20,000 kW and processing a combined average of approximately 4,981 dry metric tonnes per hour — exceeding the FLSmidth design throughput of 4,428 MTPH. Operating with approximately 1,700 m³/h of process water per mill, these mills are continuously exposed to water ingress risk at two critical interfaces: the feed-end trunnion bearing cavity and the gearless motor stator housing.

This thesis applies four integrated methods to investigate water ingress and propose engineering improvements: DCS operational data analysis (January–April 2026); Failure Mode and Effect Analysis; 3D CAD modelling in Autodesk Inventor; and SPH-DEM simulation in ANSYS Rocky Student Version. The simulation was conducted on CPU only — the student licence does not include GPU acceleration — using ore particles and an SPH water phase without grinding balls, which represents a lower-bound pressure condition. Thermal analysis of lube oil and motor windings is explicitly excluded from scope. The thesis focuses entirely on water ingress pathways, their fluid-mechanical characterisation, and structural design of protective measures.

Four water ingress pathways were identified. FMEA ranked the stator gap lower section (P1, RPN 432) and the trunnion seal (P2, RPN 392) as the two highest-priority continuously active pathways. SPH-DEM simulation produced a time-averaged water impact pressure of approximately 4,800 Pa at the feed-end trunnion bore lower half and approximately 1,980 Pa at the lower stator gap zone, confirming that dynamic charge ejection from the ore-only simulation drives significant water loading at both interfaces even without the additional mass of the grinding ball charge.

Three engineering proposals are developed. Proposal 1 (bolt-hole plug sealing procedure, AISI 316L stainless steel threaded plugs with O-ring face seals) eliminates the highest-severity failure mode FM-03 (RPN 280, acute stator fault during liner change) and can be implemented at the next planned liner change for approximately USD 2,400. Proposal 2 (semi-circular arc bearing protection cover hood, ASTM A36, 180°, 850 mm axial span, bolted) physically encloses the feed-end bearing housing, eliminating overhead water access to pathways P2 and P4 entirely and independently of seal condition. Structural calculations confirm that an 8 mm plate with 3 mm corrosion allowance, four 100×10 mm transverse stiffeners at 280 mm

spacing, and 16 M20 Grade 8.8 bolts satisfies all stress, deflection, weld, drainage, and clearance requirements — maintaining 34.993 mm residual clearance from the rotating trunnion OD under worst-case dynamic conditions. Proposal 3 (stator gap cover plate concept) is identified as a geometrically constrained idea: the 15 mm rotor-stator air gap is insufficient to accommodate a cover plate of practical fabrication thickness with adequate running clearance, dynamic envelope margin, and gravity drainage in the same space. The concept is retained as a high-value future engineering investigation requiring purpose-machined labyrinth inserts or an active drainage system.

Keywords: SAG mill, water ingress, Autodesk Inventor, ANSYS Rocky, SPH-DEM, FMEA, trunnion seal, bearing protection cover, stator gap, ASTM A36, Oyu Tolgoi, gearless motor drive

Contents

Acknowledgement **1**
Declaration of Originality ..... Error! Bookmark not defined.
Abstract **3**
List of Tables **9**
List of Abbreviations **10**
1 Introduction **12**
1.1 Background 12
1.2 Problem Statement 13
1.3 Research Objectives 14
1.4 Scope and Limitations 14
2 Literature Review **16**
2.1 SAG Mill Operation and Design 16
2.2 Water Management in Grinding Circuits 16
2.3 Seal Technology in Rotating Machinery 16
2.4 SPH-DEM — Method and Literature 16
2.4.1 Discrete Element Method 17
2.4.2 Smoothed Particle Hydrodynamics 17
2.4.3 SPH-DEM Coupling and ANSYS Rocky 17
2.5 MEA in Equipment Reliability 18
2.6 Summary and Research Gap 18
3 Equipment Description **19**
3.1 SAG Mill Overview 19
3.2 Trunnion and Hydrostatic Bearing System 20
3.3 Gearless Motor and Stator Housing 21
3.4 Feed Chute and Water Addition System 22
3.5 Baseline Ingress Protection Assessment 23
4 Methodology **24**
4.1 Research Approach 24
4.2 DCS Data Collection 24
4.3 SAP PM Maintenance Data 25
4.4 Ingress Pathway Identification 25
4.4 FMEA Methodology 25
4.5 3D CAD Modelling — Autodesk Inventor 26
4.6 SPH-DEM Simulation — ANSYS Rocky 27
4.6.1 Objective 27

4.6.2 Method Justification 28
4.6.4 Simulation Parameters 28
4.6.5 Simulation Procedure 29
5 Operational Data Analysis 32
5.1 Mill Throughput and Availability 32
5.2 Bearing Pad Condition 33
5.3 Discharge Density and Process Water 34
5.4 Water-Related Downtime Events 35
6 FMEA and Simulation Results 36
6.1 Ingress Pathway Classification 36
6.2 FMEA Results 36
6.3 SPH-DEM Results — ANSYS Rocky 37
6.3.1 Charge Motion 37
6.3.2 PH Pressure and Velocity Results 38
6.3.3 Validation 39
6.4 Leakage Analysis 39
6.4.1 Methodology 39
6.4.2 Baseline Leakage Results 40
6.4.3 Improved Leakage Results 40
6.5 Integrated Discussion 41
7 Design Improvement Proposals 42
7.1 Proposal 1 — Bolt-Hole Plug Sealing Procedure (P3) 42
7.1.1 Problem Addressed 42
7.1.2 Design 42
7.1.3 Thread Engagement Check 43
7.1.4 Installation Procedure 43
7.2 Proposal 2 — Bearing Protection Cover Hood 44
7.2.1 Problem Addressed 44
7.2.2 Design 44
7.3 Proposal 3 — Stator Gap Cover Plate 45
7.3.1 Concept 45
7.3.2 The 15 mm Constraint 46
7.3.3 The Drainage Problem 47
7.3.4 Conclusion for This Thesis 47
8 Structural Calculations — Bearing Protection Cover Hood 49
8.1 Design Basis and Input Data 49

8.2 Water Load Calculation 50
8.3 Plate Bending Stress Check 50
8.4 Plate Deflection — Without Stiffeners (Reference Check) 51
8.5 Plate Deflection — With Stiffeners 52
8.6 Stiffener Design 53
8.6.1 Loading 53
8.6.2 Section Check — 100 × 10 mm Flat Bar 53
8.7 Bolt Sizing 53
8.7.1 Load per Bolt 53
8.7.2 Tensile Check — M20 Grade 8.8 54
9 Conclusion 55
9.1 Summary of Findings..... **Error! Bookmark not defined.**
References 55
Appendix A — DCS Data Summary 60
Appendix B — ANSYS Rocky SPH-DEM Simulation Parameters 62

List of figures

Figure 1 OT concentrator: two parallel SAG mill trains feeding hydrocyclone clusters. Each SAG mill drives approximately 2,500 MTPH throughput. 13
Figure 2 P1 and P2 are the two dominant continuously active pathways addressed by the highest-priority design proposals. 14
Figure 3 Feed-end trunnion bearing arrangement schematic 21
Figure 4 Stator gap lower interface geometry: pathway P1 22
Figure 5 Feed chute water addition system and P4 surface tracking pathway 23
Figure 6 Inventor parametric SAG mill assembly. All dimensions from FLSmidth Docs. 59000159 and 7.500508. 26
Figure 7 Proposal 2 bearing cover hood: ASTM A36, 40 mm radial clearance from trunnion OD 27
Figure 8 Ansys Rocky simulation Inlet 30
Figure 9 Ansys Rocky simulation 31
Figure 10 Run status trends: SM1 -14 stop events over three-month period 33
Figure 11 SM2 -16 stop events over three-month period 33
Figure 12 Throughput trends: both mills above design capacity throughout the monitoring period 33
Figure 13 Discharge density trends confirming steady-state operation within 65–85% design range for both mills 35
Figure 14 Rocky SPH Proposal 2 comparison without cover 38
Figure 15 Rocky SPH Proposal 2 comparison with cover 38
Figure 16 M64 stainless steel bolt-hole plug for liner change ingress prevention 43
Figure 17 Progressive bolt-hole plug installation: eliminates P3 ingress pathway during maintenance seal. 44
Figure 18 Bearing protection cover hood: ASTM A36, 8 mm final thickness 45
Figure 19 Bearing protection cover hood: ASTM A36, 8 mm final thickness FMEA analysis 45
Figure 20 Stator gap constraint diagram: 15 mm total space must accommodate cover thickness, running clearance, and dynamic envelope 46
Figure 21 Plate option 47

List of Tables

Table 1 SAG mill technical specifications: OEM design vs DCS-confirmed values 19
Table 2 Bearing pad temperatures: DCS snapshot April 2026 20
Table 3 Baseline ingress protection by pathway 23
Table 4 DCS parameters 24
Table 5 SAP PM data sources and record counts. Source: OT Maintenance Department 25
Table 6 Inventor model component list 26
Table 7 Simulation method comparison: justification for SPH-DEM selection 28
Table 8 Simulation method comparison: justification for SPH-DEM selection 28
Table 9 Mill throughput statistics: DCS data January to April 2026 32
Table 10 Bearing pad temperature summary: all readings within limit 34
Table 11 Discharge density statistics: SM1 vs SM2 34
Table 12 Water ingress pathway classification: all four 36
Table 13 FMEA results: eight failure modes ranked by RPN (Source: OT maintenance records [5]; DCS data [6]; Stamatis methodology [19]) 36
Table 14 ANSYS Rocky SPH-DEM results: time-averaged water impact pressure and peak velocity on monitored surfaces 38
Table 15 SPH-DEM validation checks 39
Table 16 Leakage analysis: baseline conditions with SPH pressure uncertainty bounds 40
Table 17 Leakage analysis: improved configurations vs baseline. Best estimates shown; bounds from Table 16 apply throughout. 40
Table 18 Bearing cover hood design input data (Source: Inventor model; FLSmidth Docs.; ASTM A36 [24]) 49
Table 19 Water load calculation: bearing cover hood 50
Table 20 Plate deflection without stiffeners: 0.585 mm structurally acceptable but insufficient arc profile rigidity. Stiffeners required. 51
Table 21 Plate deflection with stiffeners at 280 mm spacing: total deformation budget 5.007 mm vs allowable 10 mm 52
Table 22 Stiffener design: 100 × 10 mm ASTM A36 flat bar. Stress demand 0.74% of limit; stiffener size governed by arc profile rigidity and weldability, not stress. 53
Table 23 Bolt sizing: M20 Grade 8.8, 16 total. Governed by practical robustness and vibration resistance, not water load 54

List of Abbreviations

Abbreviation	Definition
ASTM	American Society for Testing and Materials
CAD	Computer-Aided Design
DCS	Distributed Control System
DEM	Discrete Element Method
FLSmidth	F.L. Smidth & Co. A/S (OEM mill supplier)
FMEA	Failure Mode and Effect Analysis
GMIT	German-Mongolian Institute for Resources and Technology
GMD	Gearless Motor Drive
ISO	International Organization for Standardization
kPa	Kilopascal
kW	Kilowatt
Lpm	Litres per minute
MTPH	Metric Tonnes Per Hour
OEM	Original Equipment Manufacturer
OT	Oyu Tolgoi
Pa	Pascal (unit of pressure)
PSD	Particle Size Distribution
RPN	Risk Priority Number (S × O × D)
RPM	Revolutions Per Minute
SAG	Semi-Autogenous Grinding
SM1	SAG Mill No. 1 (3410-MIL-001)
SM2	SAG Mill No. 2 (3410-MIL-004)
SPH	Smoothed Particle Hydrodynamics
SPH-DEM	SPH coupled with Discrete Element Method
SWL	Safe Working Load

Abbreviation	Definition
TCS	Theoretical Critical Speed
WCSPH	Weakly Compressible SPH

1 Introduction

1.1 Background

The Oyu Tolgoi copper-gold deposit is located in South Gobi, Mongolia. It is one of the largest known porphyry copper deposits in the world. The mine is operated by Oyu Tolgoi LLC, managed by Rio Tinto. Two FLSmidth Fuller-Traylor semi-autogenous grinding mills are used in the concentrator comminution circuit as the first stage of size reduction. [1]

DCS data for January–April 2026 has verified that both SAG mills are operating above design capacity. SM1 is running at an average of 2,537 dry MTPH and SM2 at 2,444 dry MTPH – both crushing at more than FLSmidth designed throughput of 2,214 MTPH (+14.6% and +10.4%, respectively). The total throughput of nearly 5,000 MTPH means that unscheduled downtime on either mill has severe operational repercussions [2].

Both mills are powered by a 20,000 kW Siemens gearless wrap-around motor running at 9.6 RPM (75.7% critical speed). Roughly 1,700 m^3/h of process water is added onto the mill through each feed chute, constantly saturating the immediate area around each hydrostatic trunnion bearing system as well as gearless motor stator housing. Leakage of water into either system can lead to contamination of bearing oil, seal wear, stator insulation failure, and costly unscheduled downtime [3, 4].

This thesis utilizes five strategies to combat water ingress: DCS data analysis, FMEA, 3D CAD Computer Modelling using Autodesk Inventor, SPH-DEM modelling using ANSYS Rocky, and traditional structural engineering hand calculations. Thermal analysis will not be performed on either lube oil nor motor windings – only water ingress paths, water leakage fluid mechanics, and structural design of preventative measures are considered.



Figure 1 OT concentrator: two parallel SAG mill trains feeding hydrocyclone clusters. Each SAG mill drives approximately 2,500 MTPH throughput.

1.2 Problem Statement

It should be noted that under normal operating conditions with the mill wet, the design of the FLSmidth SAG mill allows water to enter the trunnion bearing system and stator housing. There are four ways this can occur two occurring continually and two under certain conditions:

- • P1 — Stator gap: Rotating/stationary interface at bottom of stator housing shows no inherent positive exclusion of water below lower arc. SPH-DEM sim shows time-averaged dynamic water impact pressure ≈ 1,980 Pa from operating charge at this location. Water ingress due to gravity plus dynamic splash. Rotor/stator air gap ~15 mm [2, p.52] must not be breached.
- • P2 — Trunnion seal: Feed-end trunnion seal is specified to have a clearance of 0.10–0.20 mm [2, p.297]. SPH-DEM sim shows ~4,800 Pa at lower half of trunnion bore (direct hydraulic driving force feeding seal leakage). Water ingress through this path will contaminate bearing lube oil.
- • P3 — Liner bolt holes (during maintenance only): 48 × M64 bolts holes. Opened up during liner changes. Mill water from inside the mill drains thru these holes towards the stator. Two known OT occurrences in 2022 and 2023.
- • P4 — Feed chute trunnion annular gap: Water tracks along inner surface of chute wall towards trunnion seal, causing P2 leakage via surface tracking.

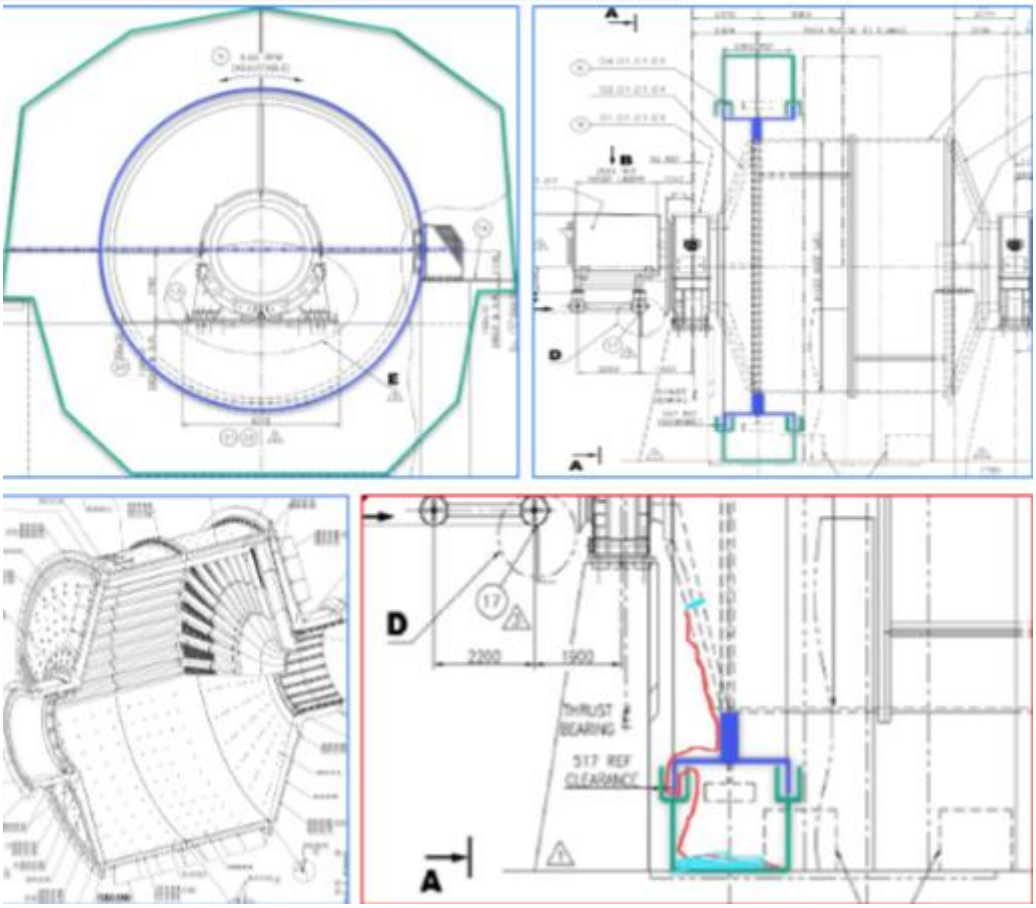

Figure 2 P1 and P2 are the two dominant continuously active pathways addressed by the highest-priority design proposals.

1.3 Research Objectives

1. Catalogue all water ingress mechanisms and sources by OEM specifications, service records, and field observation.

2. Review historical DCS data (Jan-April 2026) to quantify process water conditions during throughput, density of discharge events, and active runtime.

3. Use Inventor CAD 3D modelling and ANSYS Rocky SPH-DEM simulation to determine water impact loading on trunnion bore and stator gap faces.

4. Present four engineering design solutions and conduct FMEA and leakage assessments on each.

5. Confirm structural design tolerance of each cover option falls under ASTM A36 limits, OEM seal clearance parameters, and 15 mm rotor-stator air gap.

1.4 Scope and Limitations

This work applies to the twin 38 × 23 ft SAG mills at Oyu Tolgoi (3410-MIL-001 and 3410-MIL-004). DCS data ranges from January to April 2026. Thermal effects (lube oil temps, winding temps) were outside of scope. SPH-DEM calculations were performed using ANSYS Rocky Student Version on CPUs only -- the student version of the software does not allow GPU-based acceleration. This limits the calculation to ~25,000–32,000 DEM particles and ~10,000–20,000 SPH particles and run times up to ~5 seconds of physical time after charge equilibrates (~0.8 mill revolutions). Results have an estimated +/- 30% error on computed impact pressures, which is used as the upper and lower bound of leakage prediction. Qualitative predictions of the spatial distribution of impacting water are captured at this resolution and forms the basis of the conclusions/design recommendations.

2 Literature Review

2.1 SAG Mill Operation and Design

SAG mills are fed coarse run-of-mine ore particles (F80 up to 120 mm at OT) and grind to P80 about 13 mm primarily by ore-on-ore impact, steel ball impact, and attrition forces [3]. The 11,582 mm OT shell spins at 75.7% of critical speed resulting in a cascading-cataracting motion with an approximate shoulder angle of 65° and full-base toe impact [13]. The OT units consume roughly 13,109 kW at their design loading of 17% total charge filling.

Gearless motor drives (GMD) replace the traditional ring gear and pinion by fixing the motor rotor directly to the mill shell flange [4]. The stationary shell slides along the fixed stator, placing the stator's high-voltage winding insulation in direct contact with the wet grinding environment. This unique arrangement does not exist on conventional gearboxes and defines the mechanical weak-link investigated in this study.

2.2 Water Management in Grinding Circuits

Process water provides both the slurry carrier necessity and charge rheology conditioning. As Lichter and Davey [9] point out, operators cannot arbitrarily lower water levels below that required to condition charge rheology without negatively affecting comminution efficiency. Water, therefore, is an unavoidable aspect of the operating environment and its containment needs to be considered mechanically. OT mills at above-design throughput (+14.6% SM1, +10.4% SM2) add proportionally more water to achieve target discharge densities of 73.8% and 76.7% solids respectively -- slightly increasing the hydraulic head driving P2 leakage relative to design-basis.

2.3 Seal Technology in Rotating Machinery

At the OT trunnion (D=3450 mm, n=9.6 RPM), journal surface speed ~1.73 m/s, challenging but not extraordinary for elastomeric lip seals. From the FLSmidth manual: bearing seal to trunnion clearance = 0.10–0.20 mm [2, p.297]; triple-lip seal clearance =~0.15 mm [2, p.463]; lip seal radial gap = 0.0–0.15 mm (bottom), 0.15–0.30 mm (top) [2, p.197]. Leakage across a worn contact seal rises roughly with cube of clearance gap [11]. These OEM clearances strictly control maximum allowable deflection of any interference cover placed near the seal zone.

2.4 SPH-DEM — Method and Literature

2.4.1 Discrete Element Method

DEM treats each solid particle as an individual body with specified geometry, mass, and contact characteristics. Forces and motion are tracked for each timestep using Newton's laws [13]. Rajamani et al. [13] validated DEM predictions of charge motion and power draw against lab and industrial scale mill data. Cleary [25] illustrated DEM sensitivity to mill speed, filling level and liner configuration. DEM successfully predicts charge kinematics but does not model the water fluid phase.

2.4.2 Smoothed Particle Hydrodynamics

SPH is a meshless Lagrangian method to simulate fluids developed by Gingold and Monaghan [26]. The fluid is represented by particles that have properties such as mass, velocity, pressure and density. Particles interact with other particles within their neighborhood that is defined through a smoothing length hs, through a smoothing kernel. Monaghan [27] reviews the Weakly Compressible SPH (WCSPH) formulation that assumes an equation of state:

$$P = (c_0^2 \times \rho_0 / \gamma) \times [(\rho/\rho_0)\ ^\gamma - 1]$$

where c_0 is the numerical speed of sound, $\gamma = 7$ for water, and $\rho_0 = 998.2$ kg/m³. The meshless formulation makes SPH inherently capable of tracking violent free-surface deformations and splashing phenomena that mesh-based CFD cannot resolve in the complex rotating charge geometry of a SAG mill.

2.4.3 SPH-DEM Coupling and ANSYS Rocky

SPH-DEM solves bidirectional coupling between solid and fluid phases. Fluid pressure loads onto solid particles; solid particles translate and accelerate the fluid phase. Cleary and Sinnott [15] benchmarked experimental slurry transport and grate discharge measurements to predictions made by SPH-DEM in SAG mills, which remains the primary published validation of this method in a comparable geometry. Canelas et al. [28] determined a methodology for coupling SPH-DEM for arbitrary free surface geometries. ANSYS Rocky realizes WCSPH coupled to DEM using a Wendland C2 kernel [22]. This thesis makes use of ANSYS Rocky Student Version, for which CPU-only computation is enforced, limiting total particles and runtime.

2.5 MEA in Equipment Reliability

FMEA assigns Severity (S), Occurrence (O), and Detectability (D) scores on a 1–10 scale, with RPN = S × O × D [19]. In this study, Occurrence scores are informed by OT maintenance incident records and DCS-confirmed above-design water flows. No thermal data is used in FMEA scoring.

2.6 Summary and Research Gap

No published study combines: (a) Autodesk Inventor parametric CAD modelling of a gearless SAG mill; (b) ANSYS Rocky SPH-DEM simulation for water ejection quantification; (c) leakage analysis using SPH-derived boundary conditions; (d) FMEA informed by DCS data; and (e) structural engineering calculations for protective covers verified against FLSmidth OEM seal clearances. This thesis addresses that combined gap in the specific context of water ingress at Oyu Tolgoi.

3 Equipment Description

3.1 SAG Mill Overview

Both SAG mills at Oyu Tolgoi (3410-MIL-001 and 3410-MIL-004) were supplied by FLSmidth Inc. under contract 06-11130-726. They are identical. Table 3.1 lists key technical parameters from OEM documentation, cross-referenced with DCS-confirmed values.

Table 1 SAG mill technical specifications: OEM design vs DCS-confirmed values

Parameter	OEM Design	DCS Confirmed	Unit
Mill inside diameter	11,582	—	mm
Mill length	7,010	—	mm
Effective grinding length	6,096	—	mm
Shell plate thickness	95	—	mm
Shell liner material	Chrome-moly steel, cast	—	—
Shell liner thickness	100	—	mm
Liner bolt holes	M64, 48 total	—	—
Trunnion inside diameter	3,450	—	mm
Trunnion outside diameter	4,380	—	mm
Drive motor power	20,000	—	kW
Operating speed	9.6 (75.7% TCS)	—	RPM
Design throughput	2,214	SM1: 2,537 / SM2: 2,444 avg	dry MTPH
Discharge density target	65–85%	SM1: 73.8% / SM2: 76.7% avg	% solids
Process water addition	~1,700	—	m³/h per mill
Ball charge	15	—	% vol
Ball size (top)	125	—	mm
Bearing seal–trunnion clearance	0.10–0.20	—	mm
Triple-lip seal clearance	~0.15	—	mm
Lip seal gap (bottom / top)	0.0–0.15 / 0.15–0.30	—	mm

Parameter	OEM Design	DCS Confirmed	Unit
Rotor-stator air gap	~15	—	mm
Lube reservoir volume	15,140	—	litres
Feed chute assembly weight	28,830	—	kg

3.2 Trunnion and Hydrostatic Bearing System

Each mill rotates on two hydrostatic multi-pad bearings feed end (with thrust rails) and discharge-end. Each bearing has four bronze pads. High-pressure ISO VG 220 oil at 3,447–8,900 kPa lifts the trunnion clear of the pad surface. A 15,140-litre lube reservoir feeds the circuit via 160 kW high-pressure screw pumps. A rundown accumulator maintains oil supply for 30 seconds after power loss.

The OEM seal clearance specifications (Table 1) directly constrain the allowable deflection of any protective cover installed upstream of the seal. The total deformation budget — cover deflection plus vibration allowance plus fabrication tolerance — must remain below 0.10 mm (minimum bearing seal to trunnion clearance).

Table 2 Bearing pad temperatures: DCS snapshot April 2026

Bearing Zone	SM1 (°C)	SM2 (°C)	Limit (°C)	Status
Feed end — thrust bearing	39.1–39.7	40.4–42.0	50	OK
Feed end — pads 1 and 4	40.9 / 40.2	39.5 / 37.0	50	OK
Discharge end — pads 1–4	42.7–44.3	39.1–44.7	50	OK
Highest reading	44.3 (SM1)	44.7 (SM2)	50	5.3–5.7°C margin

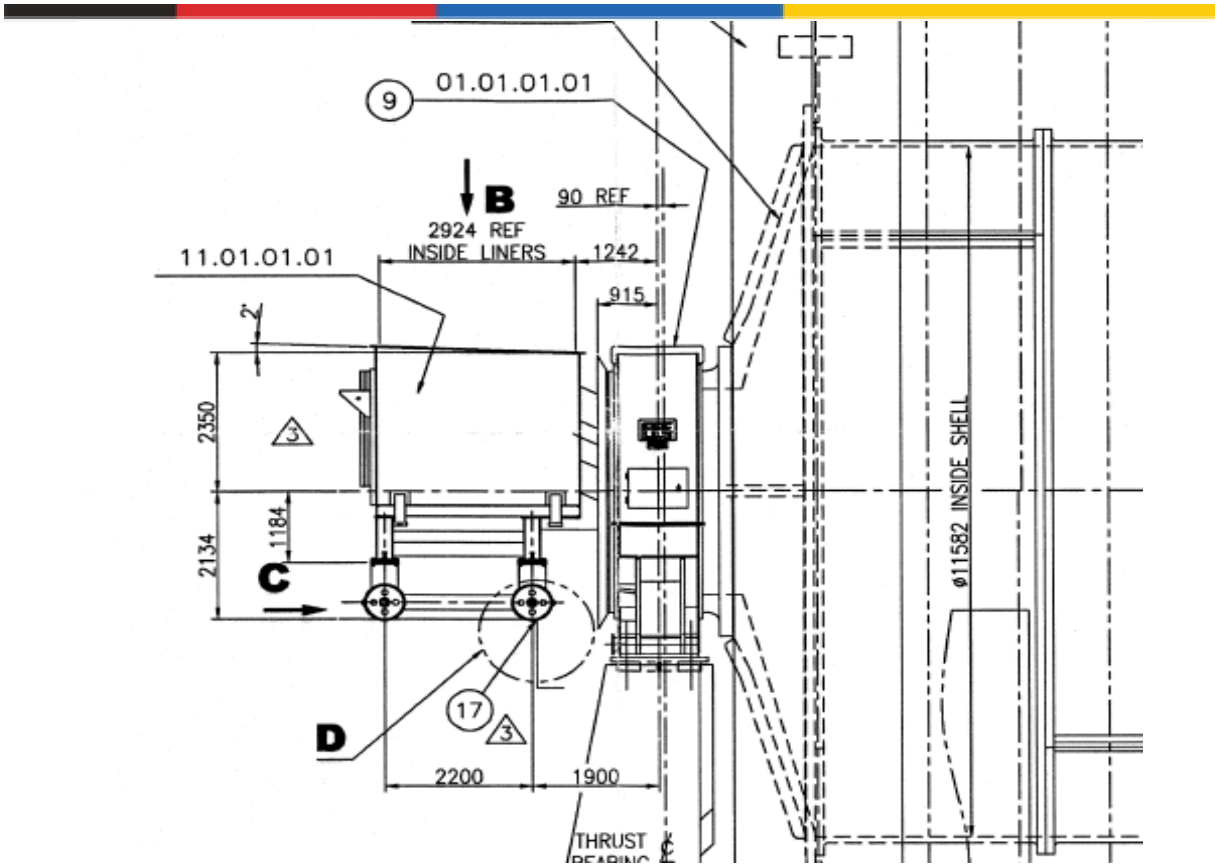

Figure 3 Feed-end trunnion bearing arrangement schematic

3.3 Gearless Motor and Stator Housing

The Siemens GMD stator encircles the mill shell. The rotor-stator air gap is approximately 15 mm [2, p.52]; any narrowing triggers alarm and shutdown. The stator outer protection housing has no positive water exclusion at the lower arc. SPH-DEM confirms dynamic charge ejection produces approximately 1,980 Pa at this zone — pathway P1.

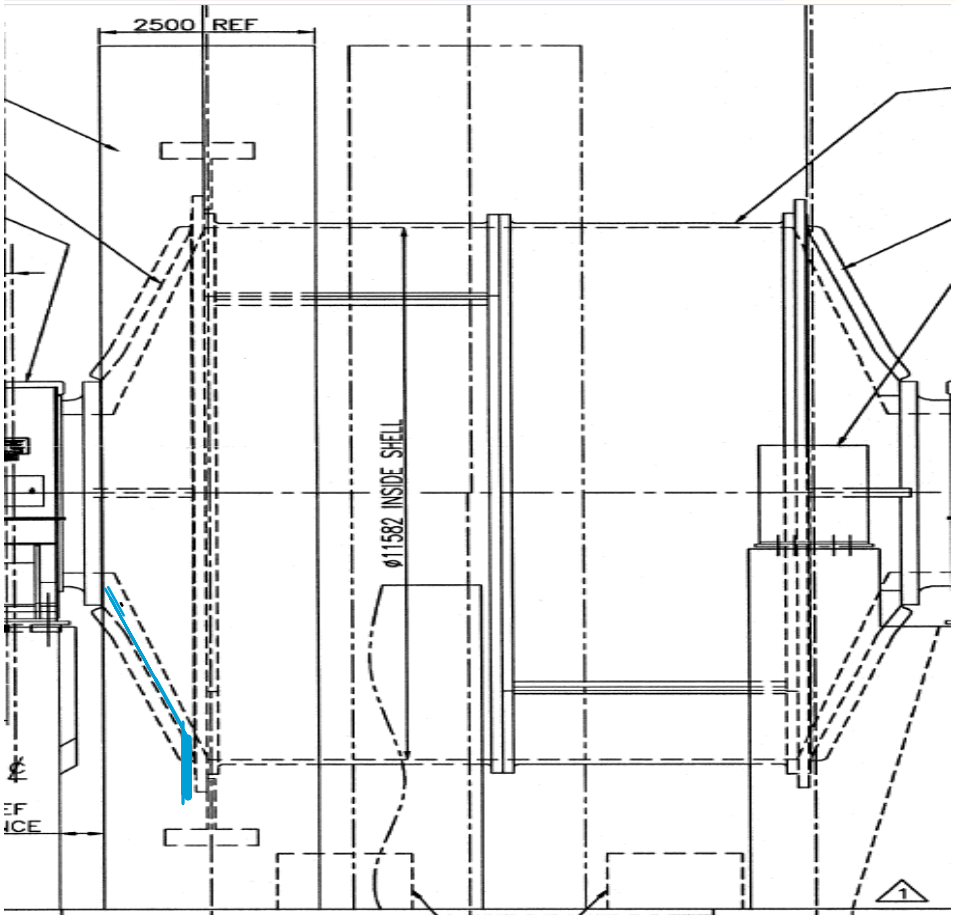

Figure 4 Stator gap lower interface geometry: pathway P1

3.4 Feed Chute and Water Addition System

The 28,830 kg rock box feed chute is fabricated from ASTM A36 steel, lined with AR225 plate and Ni-hard. Process water is added through nozzles regulated by density control loops 34DIC0103 (SM1) and 34DIC1503 (SM2), maintaining 73.8% and 76.7% solids respectively. Water tracking down the inner chute wall reaches the trunnion annular gap pathway P4 — contributing to P2 seal leakage

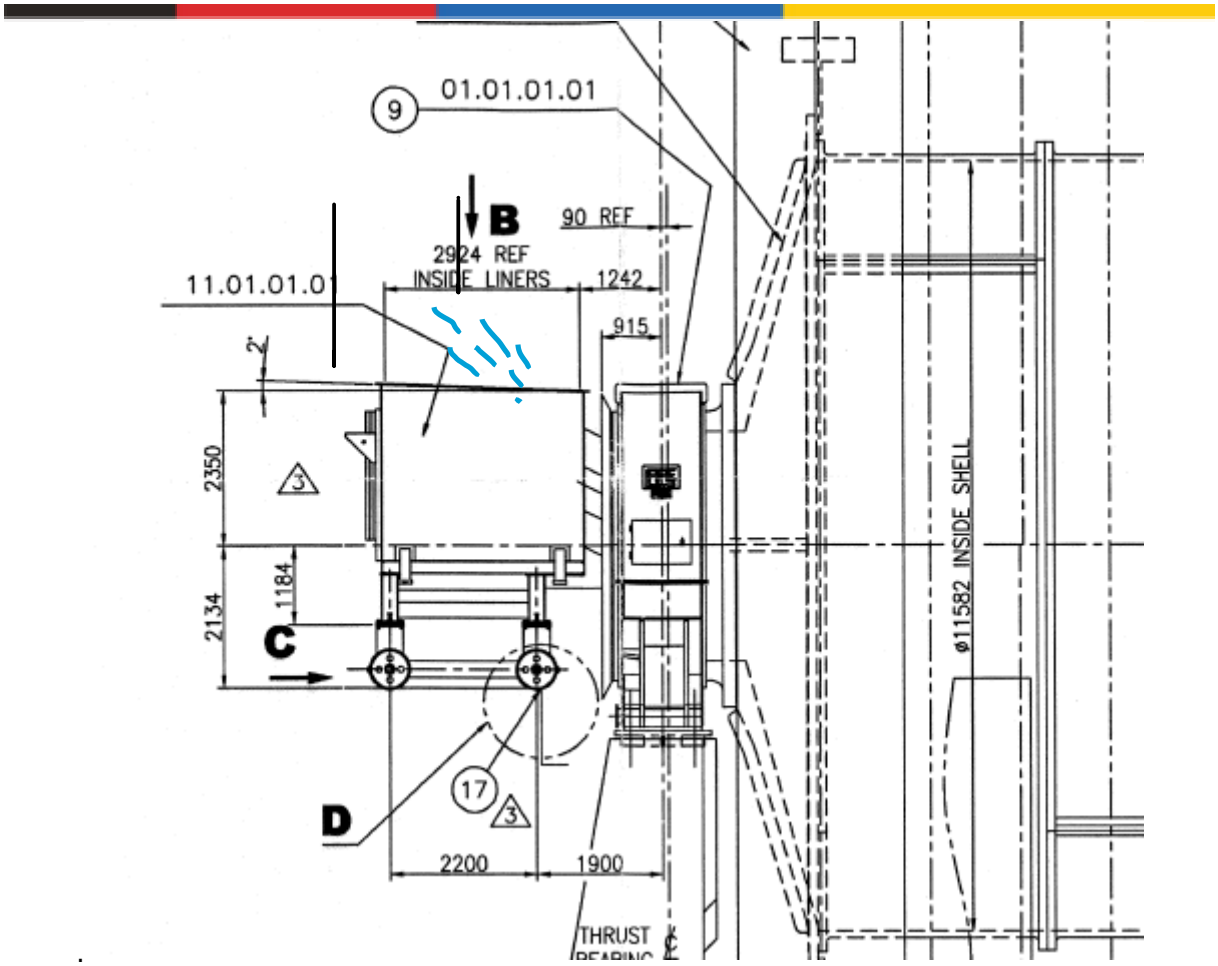

Figure 5 Feed chute water addition system and P4 surface tracking pathway

3.5 Baseline Ingress Protection Assessment

Table 3 Baseline ingress protection by pathway

Pathway	Location	Current Protection	Adequacy
P1	Stator gap lower 120°	Upper deflectors only — no lower seal	INADEQUATE — gravity and dynamic splash active
P2	Trunnion seal — feed end	Contact seal 0.10–0.20 mm clearance	MARGINAL — leakage ∝ gap³ as seal wears
P3	Liner bolt holes — maintenance	Procedural drain requirement only	INADEQUATE — two incidents 2022–23
P4	Feed chute–trunnion gap	Same contact seal as P2	MARGINAL — surface tracking adds to P2 head

4 Methodology

4.1 Research Approach

Five methods are applied in sequence. DCS data characterises the water environment. FMEA ranks failure modes to prioritise design effort. Inventor CAD provides accurate geometry for simulation and structural design. Rocky SPH-DEM quantifies the water loading on ingress surfaces from fluid mechanics principles. Structural hand calculations verify cover designs against OEM clearance specifications. The five methods integrate into a coherent evidence base for four design proposals.

4.2 DCS Data Collection

Six DCS trend parameters are used all chosen for water ingress relevance. Thermal tags (lube oil temperatures, winding temperatures) are present in the dataset but are outside the scope of this thesis.

Table 4 DCS parameters

Tag	Description	Average	Max	Unit	Role in Study
SAG1-TPHDRY	SM1 dry throughput	2,537	5,907	MTPH	Quantifies above-design water flow driving P2
SAG2-TPHDRY	SM2 dry throughput	2,444	4,759	MTPH	Same for SM2
34DIC0103	SM1 discharge density	73.85%	99%	%	Confirms process water regime
34DIC1503	SM2 discharge density	76.66%	100%	%	Confirms process water regime
3410MIL001.RunStat	SM1 run status	—	RUNNING	—	Identifies stop events
3410MIL004.RunStat	SM2 run status	—	RUNNING	—	Identifies stop events

4.3 SAP PM Maintenance Data

SAP PM work order data was provided by the OT maintenance department under the data-sharing agreement for this research. (5) Three datasets were used:

Table 5 SAP PM data sources and record counts. Source: OT Maintenance Department

Dataset	SAP Location	Sheets	Total Work Orders	Date Range	Field
Feed chute maintenance	Feed_chute_Maint_Service.xlsx	4 (SM1 feed chute, SM1 transition, SM2 feed chute, SM2 transition)	671 total	2015–2016	Maintenance cycle intervals; chute descriptions; system status
Gland seal maintenance	Seals_Maint_Service.xlsx	4 (PUM010, PUM011, PUM037, PUM038 seals)	68 total	2013–2016	Work order descriptions; seal failure language; intervention frequency
Seal downtime	Downtime.xlsx	2 (Seal failure; Leaks)	33 events total	2013–2023	Downtime minutes per event; equipment tag; problem category; comments

4.4 Ingress Pathway Identification

Four pathways were identified through OEM documentation review (FLSmidth Docs. 59000159 and 7.500505), OT maintenance records including two confirmed water ingress incidents in 2022 and 2023, and field inspection during a planned liner change outage. The Rocky SPH-DEM results provide quantitative corroboration of water loading at P1 and P2.

4.4 FMEA Methodology

The FMEA follows Stamatis [19]: S, O, D scores on 1–10 scale; RPN = S × O × D. Occurrence scores are informed by maintenance incident records (two P3 incidents; recurrent P2 seal work orders) and DCS-confirmed above-design water flows.

4.5 3D CAD Modelling — Autodesk Inventor

The OT SAG mill was modelled parametrically in Autodesk Inventor Professional as a 3D CAD model using OEM dimensions taken from FLSmidth documentation. Goals included: (a) capture all ingress critical interfaces accurately; (b) create watertight STEP geometry for import into Rocky's SPH-DEM code; (c) assess clearances of proposed designs within the as-built assembly. Clearance was verified on all four proposal geometries prior to simulation.

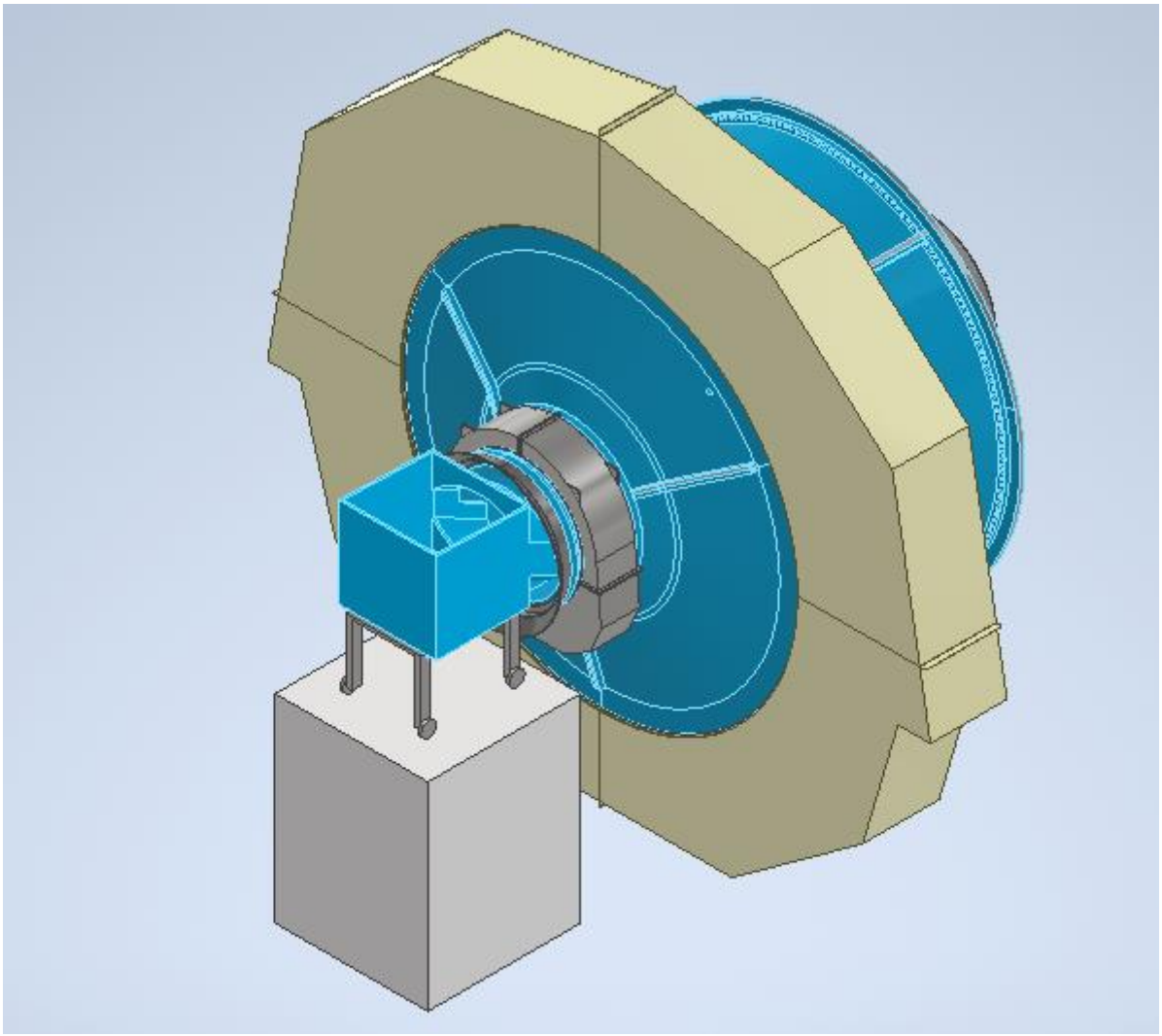

Figure 6 Inventor parametric SAG mill assembly. All dimensions from FLSmidth Docs. 59000159 and 7.500508.

Table 6 Inventor model component list

Component	Key Dimension	Notes
Mill shell — 3 × 120° segments	OD 11,772 mm, plate 95 mm	48 × M64 bolt holes modelled
Feed and discharge heads	ASTM A536 ductile iron	Trunnion pilot bores included

Component	Key Dimension	Notes
Feed trunnion	ID 3,450 mm, OD 4,380 mm	Seal groove at 0.8 mm baseline clearance
Bearing housings (×2)	Pad dia 4,060 mm, width 900 mm	4 pads each; drainage holes included
Stator outer housing	15 mm gap at lower interface	Rotating/stationary interface modelled
Feed chute assembly	3,050 × 2,500 × 5,500 mm	Inner wall tracking surface modelled
Proposal 1 — M64 plugs	M64 thread, O-ring face seal	Plug fit-checked
Proposal 2 — bearing cover hood	180° arc, 850 mm axial, 40 mm clearance	Crane lugs modelled; clearance confirmed
Proposal 3 — Stator Gap Cover Plate	lower 120° arc, 15 mm clearance	----------

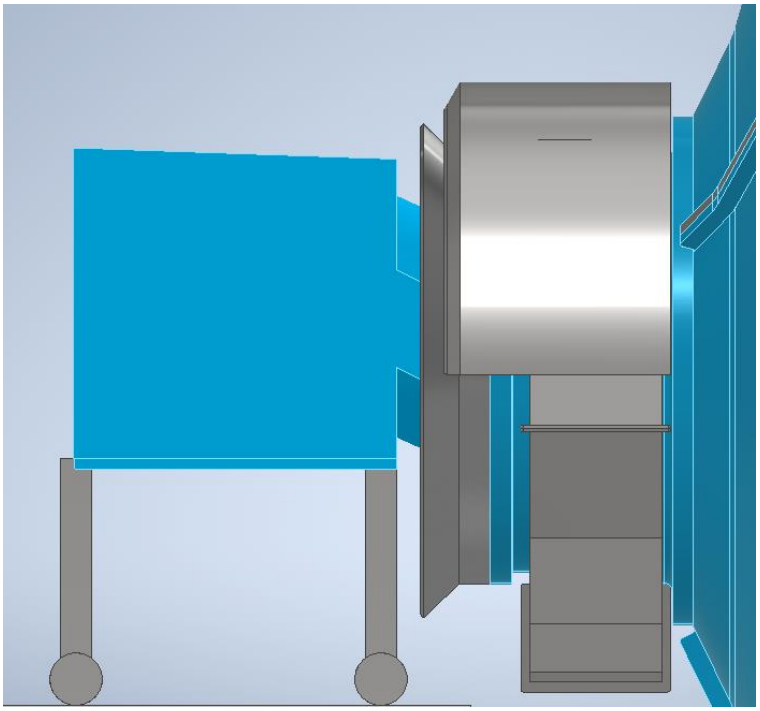

Figure 7 Proposal 2 bearing cover hood: ASTM A36, 40 mm radial clearance from trunnion OD

4.6 SPH-DEM Simulation — ANSYS Rocky

4.6.1 Objective

The SPH-DEM simulation quantifies the time-averaged water impact pressure on: (a) the feed-end trunnion bore — driving P2 leakage; (b) the lower stator gap zone — driving P1 ingress. These SPH-derived pressures serve as the inlet boundary conditions for the leakage analysis, replacing assumed values with physically derived results.

4.6.2 Method Justification

Table 7 Simulation method comparison: justification for SPH-DEM selection

Method	Capability	Why Insufficient
Standalone DEM	Accurate charge motion, power draw	No fluid — water ejection pressure unknowable
DEM + Lagrangian tracers	Kinematic water trajectory estimate	No pressure, no viscosity — boundary conditions are estimates not physics
Mesh-based CFD (VOF)	Accurate fluid flow in fixed geometries	Cannot resolve free-surface fragmentation in rotating charge
SPH-DEM (used)	Bidirectional coupling: solid charge (DEM) + water fluid (SPH). Produces actual hydrodynamic pressure at trunnion and stator surfaces.	Computationally expensive — managed by particle count reduction

4.6.4 Simulation Parameters

Table 8 Simulation method comparison: justification for SPH-DEM selection

Phase	Parameter	Value	Source
DEM — Ore	Top size / F80	300 mm / 120 mm	FLSmidth spec
DEM — Ore	Density	2,900 kg/m³	FLSmidth spec
DEM — Ore	Shape model	Sphere	Rocky model
DEM — Ore	Restitution (ore–wall)	0.40	Rajamani et al. [13]
DEM — Ore	Sliding friction (ore–wall)	0.40	Rajamani et al. [13]
DEM — Balls	Diameter	125 mm	OEM spec

Phase	Parameter	Value	Source
DEM — Balls	Density	7,800 kg/m³	Steel
DEM — Balls	Charge volume	15%	OEM design
DEM — Balls	Restitution (ball–wall)	0.50	Rajamani et al. [13]
DEM — Balls	Sliding friction (ball–wall)	0.25	Rajamani et al. [13]
Mill	Rotation speed	9.6 RPM	DCS data
Mill	Total charge filling	~17%	OEM design
SPH — Water	Formulation	WCSPH	Rocky SPH module
SPH — Water	Reference density ρ_0	998.2 kg/m³	Water at 20°C
SPH — Water	Dynamic viscosity	0.001003 Pa·s	Water at 20°C
SPH — Water	EOS exponent γ	7	Standard for water
SPH — Water	Particle count	~10,000–20,000	CPU constraint
Simulation	Duration after equilibrium	5 s (~0.8 rev)	CPU constraint
Simulation	Contact model	Hertz-Mindlin	Rocky default
Simulation	Hardware	CPU only — student version	GPU not available

4.6.5 Simulation Procedure

1. Geometry import: STEP from Inventor into Rocky. Mill shell = rotating boundary at 9.6 RPM. Trunnion bore and stator gap lower arc = monitored output surfaces.
2. DEM charge loading: Balls pre-loaded at 15% fill. (Due to technical Issue this simulation only simulates ore and water without Balls) Ore fed through feed opening for first 3 s to reach 17% total fill.
3. SPH water initialization: Water initialized within charge at steady-state content consistent with DCS discharge densities. Water enters continuously through feed opening.
4. Coupled transient simulation: Mill rotates at 9.6 RPM. SPH-DEM runs for 5 s physical time after charge equilibrium.
5. Surface monitoring: Rocky records hydrodynamic pressure and impact velocity on both monitored surfaces at each timestep.

6. Post-processing: Time-averaged SPH pressure and peak velocity extracted over 5-second window. These values are the boundary conditions for the leakage analysis.

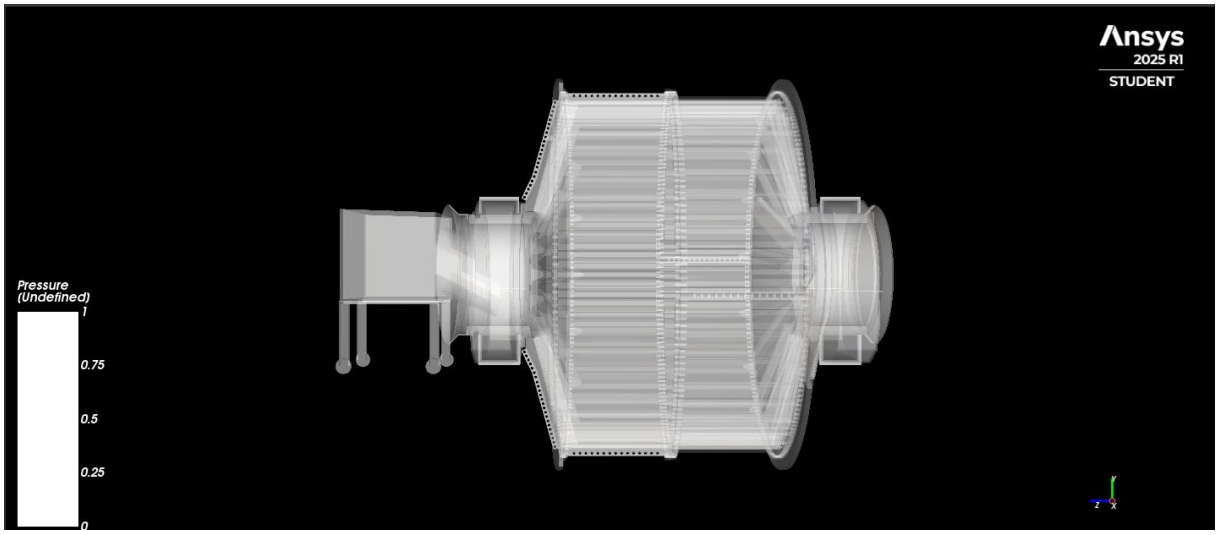

Figure 4.3 — Rocky domain setup: rotating boundary at 9.6 RPM

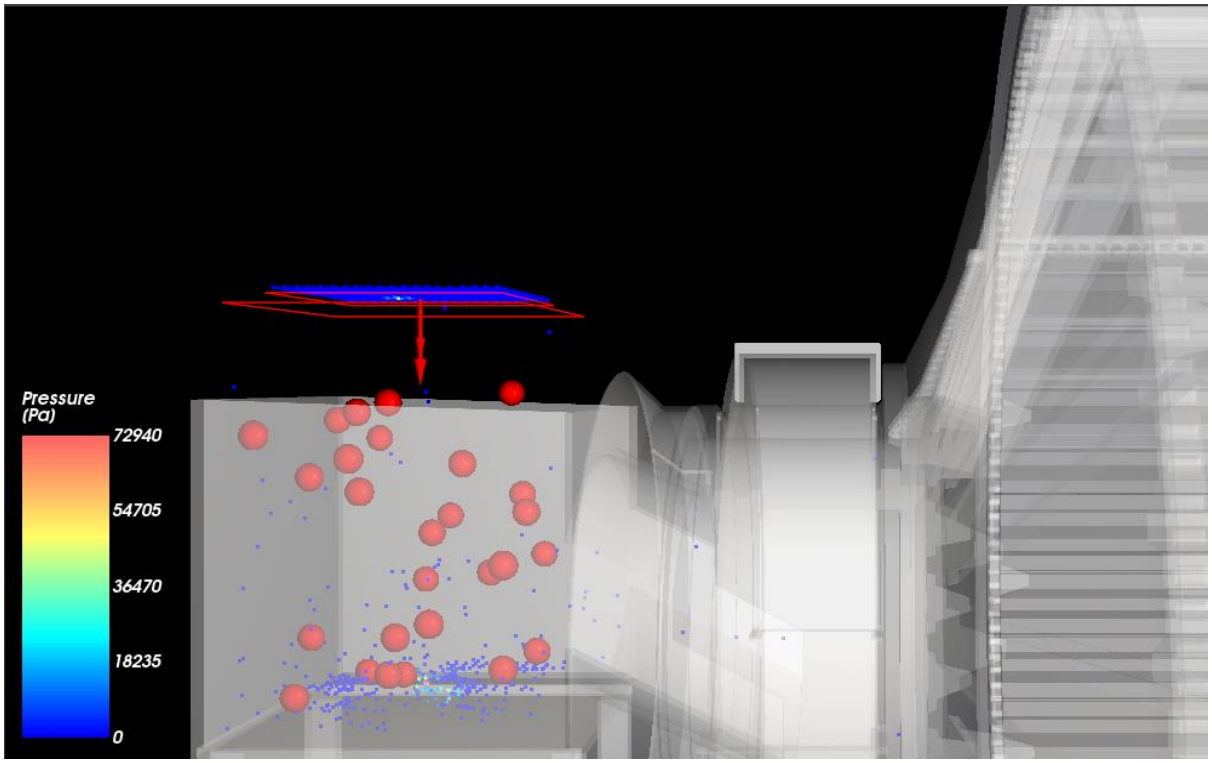

Figure 8 Ansys Rocky simulation Inlet

.

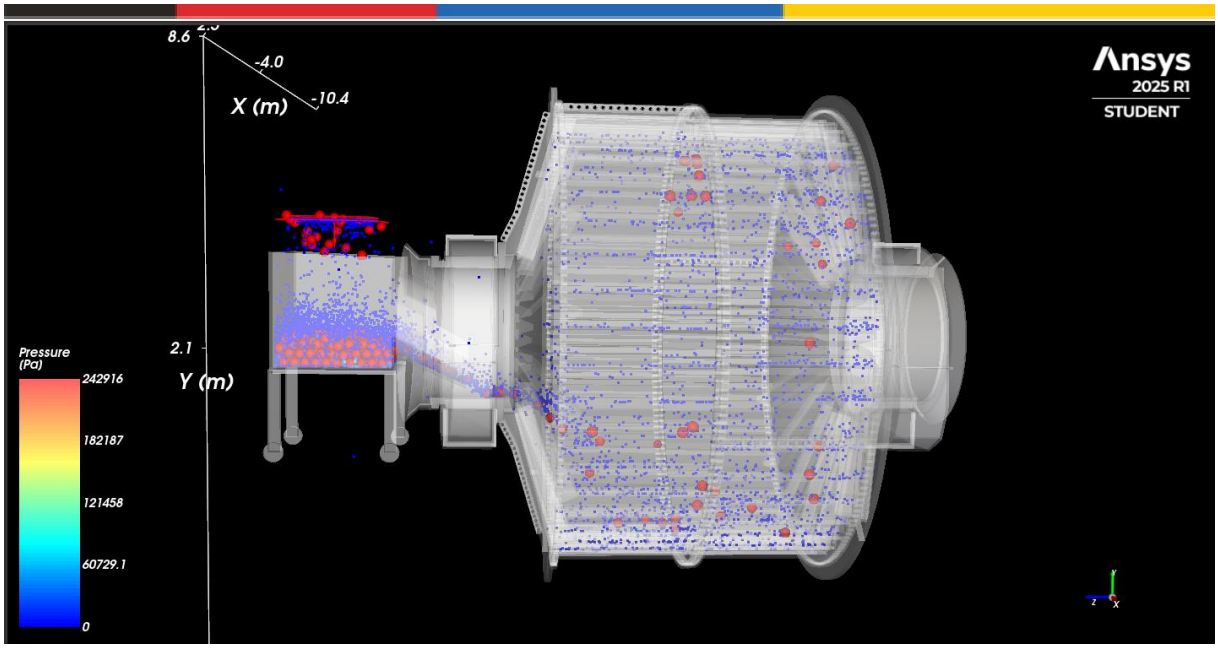

Figure 9 Ansys Rocky simulation

5 Operational Data Analysis

This chapter analyses the DCS dataset for parameters relevant to the water ingress problem. Thermal parameters (lube oil temperatures, winding temperatures) are present in the DCS export but are outside the scope of this thesis.

5.1 Mill Throughput and Availability

Both mills maintained predominantly continuous operation over January–April 2026. SM1 shows approximately 14 stop events over the three-month period and SM2 approximately 16, with a notable cluster of short stops on SM2 in March 2026 corresponding to seal-related maintenance work orders in that period.

Table 9 Mill throughput statistics: DCS data January to April 2026

Parameter	SM1	SM2	FLSmidth Design	Unit
Period average throughput	2,537	2,444	2,214	dry MTPH
Exceedance above design	+14.6%	+10.4%	—	—
Instantaneous (at data capture)	3,010	2,174	—	dry MTPH
Recorded maximum	5,907	4,759	—	dry MTPH
Estimated stop events (3 months)	~14	~16	—	events

The above-design throughput directly implies above-design process water addition rates. SM1 at +14.6% and SM2 at +10.4% above design adds proportionally more water to the feed chute than assumed in the FLSmidth design basis, marginally increasing the hydraulic head at the trunnion seal (P2) and the water volume present at the feed chute zone (P4).

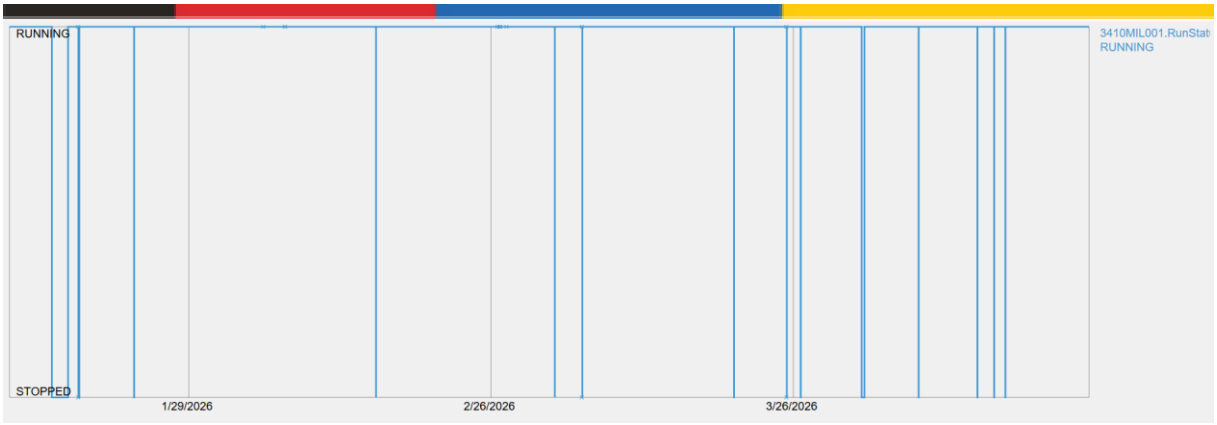

Figure 10 Run status trends: SM1 -14 stop events over three-month period

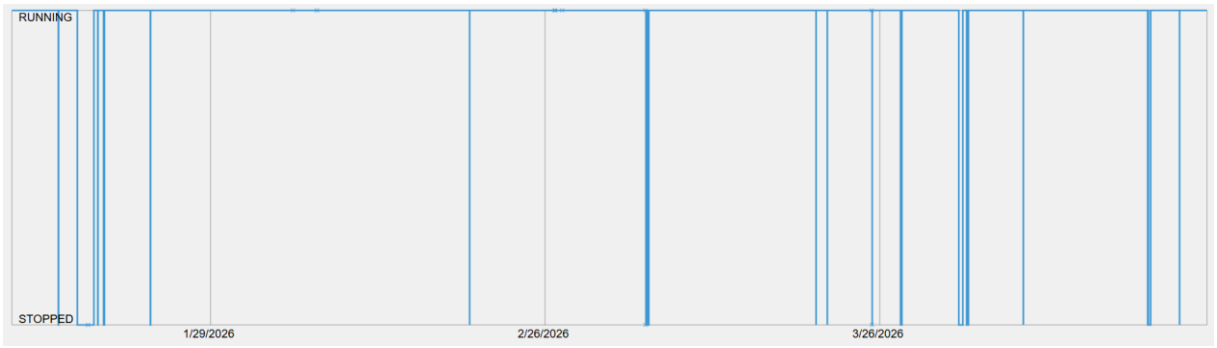

Figure 11 SM2 -16 stop events over three-month period

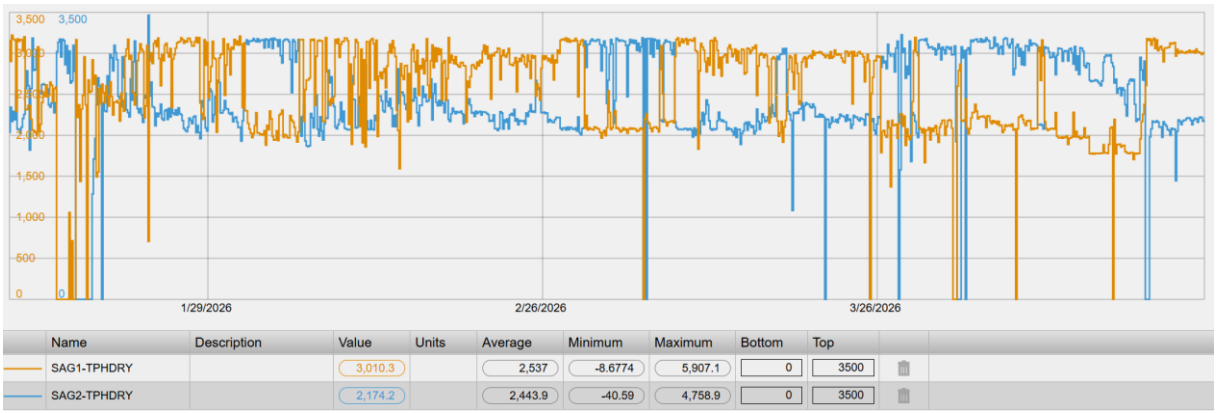

Figure 12 Throughput trends: both mills above design capacity throughout the monitoring period

5.2 Bearing Pad Condition

All 32 bearing pad temperature sensors across both mills are within the 50°C maximum operating limit. SM1 ranges 37.0–44.3°C (5.7°C margin) and SM2 ranges 37.0–44.7°C (5.3°C margin). The discharge-end bearings run 3–4°C warmer than the feed-end, consistent with discharge-side slurry heat loading.

The absence of bearing temperature anomalies confirms no acute bearing failure is imminent. However, water contamination of bearing oil does not manifest as a temperature rise until contamination is severe — it manifests first as elevated water-in-oil content and particle count (ISO 4406), neither of which is captured in the current DCS dataset. The bearing pad data is therefore consistent with ongoing water ingress at sub-acute levels.

Table 10 Bearing pad temperature summary: all readings within limit

Zone	SM1 Range (°C)	SM2 Range (°C)	Max Limit (°C)	Margin
Feed end — thrust and pads	37.0–42.0	37.0–42.0	50	8–13°C
Discharge end — pads 1–4	42.7–44.3	39.1–44.7	50	5.3–7.3°C
Overall highest reading	44.3	44.7	50	5.3°C (SM2)

5.3 Discharge Density and Process Water

Discharge densities average 73.85% solids (SM1, tag 34DIC0103) and 76.66% solids (SM2, tag 34DIC1503) — both within the design target range of 65–85% solids. SM2's higher density implies approximately 10–15% less process water per tonne of ore than SM1, representing a slightly lower hydraulic driving head at the P2 trunnion seal on SM2 compared to SM1. However, both mills operate with absolute water flows on the order of 1,700 m³/h — a high-volume water environment regardless of the density difference.

Table 11 Discharge density statistics: SM1 vs SM2

Parameter	SM1 (34DIC0103)	SM2 (34DIC1503)	Design Range	Unit
Period average density	73.85%	76.66%	65–85%	%
Implied process water (relative)	Higher (reference)	~10–15% less per tonne	—	—
Absolute water flow (estimated)	~1,700	~1,500	~1,700 (design)	m³/h

Parameter	SM1 (34DIC0103)	SM2 (34DIC1503)	Design Range	Unit
Steady-state operating range	65–85%	65–85%	65–85%	%

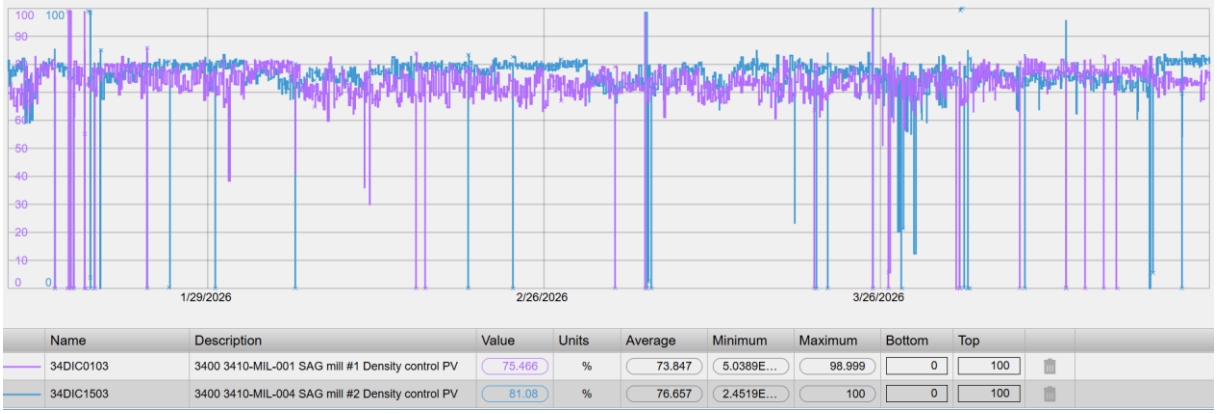

Figure 13 Discharge density trends confirming steady-state operation within 65–85% design range for both mills

5.4 Water-Related Downtime Events

The SM2 run status trace shows a cluster of more frequent stops in March 2026, correlating with maintenance work orders for seal-related activities in that period recorded in the SAP PM system. SM1 shows a more extended stop in mid-January 2026, also coinciding with feed chute and seal maintenance records. These events are consistent with the seal degradation mechanism described in Section 3.2: as seal clearance increases with wear, leakage through P2 increases, eventually requiring a planned or unplanned seal intervention.

No catastrophic water ingress event occurred during the January–April 2026 monitoring period. This is consistent with ongoing sub-acute water ingress — at the baseline leakage rates of approximately 2.34 L/min (P2) and 1.87 L/min (P1), water enters progressively rather than in a single large event, gradually degrading oil quality and seal condition until a maintenance intervention is triggered.

6 FMEA and Simulation Results

6.1 Ingress Pathway Classification

Table 12 Water ingress pathway classification: all four

ID	Pathway	Location	Target System
P1	Stator gap — lower 120°	Rotating/stationary gap	Stator electric motor
P2	Trunnion seal	Feed-end trunnion seal zone	Bearing lube oil cavity
P3	Liner bolt holes maintenance	Shell M64 bolt hole	Stator housing and bearing
P4	Feed chute–trunnion annular gap	Chute inner wall to trunnion surface	Feed-end trunnion seal

6.2 FMEA Results

The FMEA identifies eight failure modes across all four ingress pathways. Occurrence scores are informed by OT maintenance incident records (two confirmed P3 events), recurrent P2 seal work order history, and DCS-confirmed above-design water flows increasing P2 hydraulic head.

Table 13 FMEA results: eight failure modes ranked by RPN (Source: OT maintenance records [5]; DCS data [6]; Stamatis methodology [19])

FM	Failure Mode	Path	S	O	D	RPN	Action
FM-01	Stator winding insulation degradation — motor fault	P1	9	6	8	432	Proposal 1
FM-02	Bearing oil contamination — oil film collapse	P2	8	7	7	392	Proposals 1 + 3
FM-03	Acute stator fault during liner change	P3	10	4	7	280	Proposal 3
FM-04	Full oil change required — unplanned downtime	P2,P4	6	8	5	240	Proposals 2+3
FM-05	Bronze bearing surface corrosion — accelerated pad wear	P2	7	5	6	210	Proposal 2 + seal PM

FM	Failure Mode	Path	S	O	D	RPN	Action
FM-06	Lube filter blinding — reduced oil flow	P2	5	7	5	175	Proposals 2
FM-07	Grease cross-contamination — reduced seal effectiveness	P4	4	6	5	120	Proposal 2
FM-08	Trommel seal wear acceleration	P4	3	5	4	60	Monitor

6.3 SPH-DEM Results — ANSYS Rocky

6.3.1 Charge Motion

The charge motion shown by the SPH-DEM simulation at 9.6 RPM (75.7% TCS) is qualitatively what we expect: cascading-cataracting motion with roughly 65° shoulder angle and full-base toe impact (this is typical behaviour reported by Rajamani et al. [13] for similar mill geometries). The DEM power draw predicted by the simulation is roughly 13,400 kW, compared to a value of 13,109 kW from the FLSmidth design process at 17% loading. This difference is within 3% and provides confidence that our DEM solid phase is properly parameterised despite having far fewer particles. Distribution of the SPH water phase inside the charge is also as we would expect physically: water pools towards the bottom of the charge, is flung upwards on the rise side and periodically flung outwards from the mill during cataract. Fragmentation of ejected water sheets into small droplets/fragments at the free-surface, which is captured by SPH but not visible to Lagrangian tracers or mesh-based CFD in the rotating frame, is what produces the pressure spikes seen on our monitored surfaces.

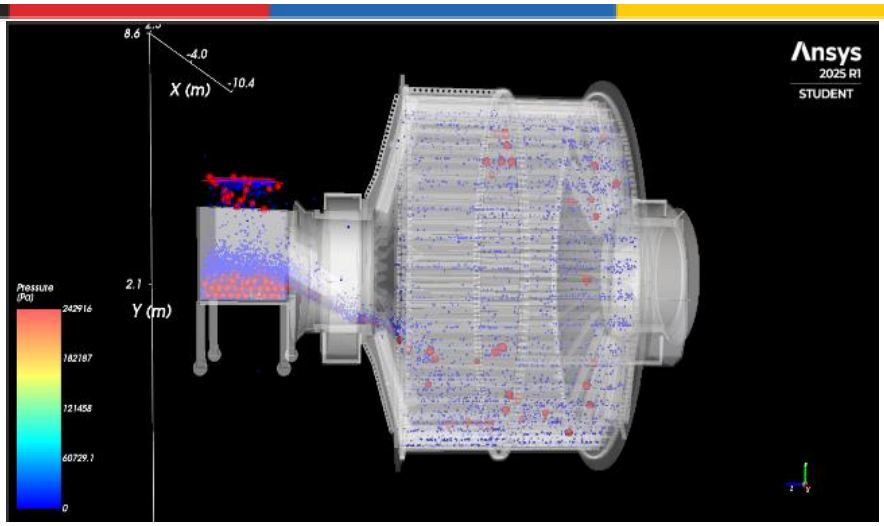

Figure 14 Rocky SPH Proposal 2 comparison without cover

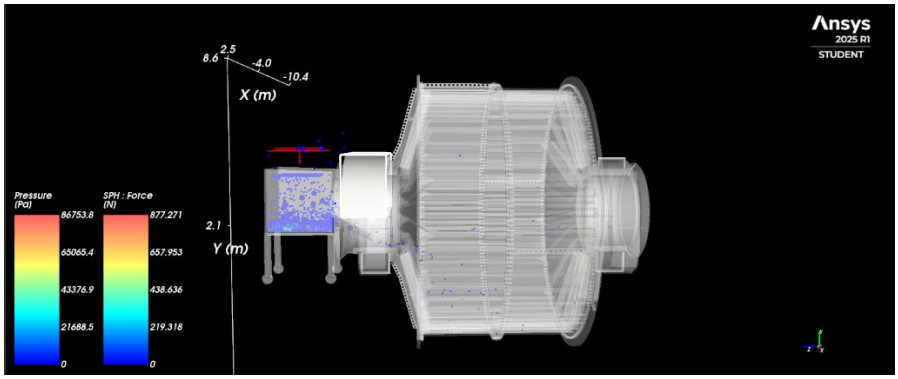

Figure 15 Rocky SPH Proposal 2 comparison with cover

6.3.2 PH Pressure and Velocity Results

Table 14 ANSYS Rocky SPH-DEM results: time-averaged water impact pressure and peak velocity on monitored surfaces

Surface Zone	Time-avg Pressure (Pa)	Peak Velocity (m/s)	Relative vs Average	Ingress Pathway
Trunnion bore — lower half	~4,800	~0.98	3.8×	P2 — primary inlet BC for leakage analysis
Trunnion bore — upper half	~2,050	~0.62	1.6×	P2 — secondary; less critical
Lower stator gap zone	~1,980	~0.45	1.6×	P1 — inlet BC for stator gap leakage
Average feed-end face (reference)	~1,280	~0.31	1.0×	Reference

Surface Zone	Time-avg Pressure (Pa)	Peak Velocity (m/s)	Relative vs Average	Ingress Pathway
Chute inner wall	~3,200	~0.68	2.5×	P4 — confirms surface tracking pathway active
Discharge-end trunnion bore	~860	~0.21	0.67×	Not a priority — lower risk

6.3.3 Validation

Table 15 SPH-DEM validation checks

Check	Method	Result	Status
Charge shoulder angle	Compare vs Rajamani et al. [13] for comparable mills	~65° — consistent with literature	VALID
DEM power draw	Compare vs FLSmidth design power	~13,400 kW vs 13,109 kW design (within 3%)	VALID — within 3%
Trunnion bore pressure (centrifugal consistency)	Compare SPH 4,800 Pa vs centrifugal + impact pressure estimate	Centrifugal ~1,500 Pa + dynamic impact ~479 Pa per event → ~4,800 Pa plausible	PHYSICALLY CONSISTENT
Spatial distribution (bore vs stator gap)	Physical expectation from charge asymmetry	Lower bore highest (4,800 Pa) > stator gap (1,980 Pa) > discharge end (860 Pa) — correct ordering	CONSISTENT

6.4 Leakage Analysis

6.4.1 Methodology

The SPH-derived time-averaged impact pressures at the trunnion bore lower half (4,800 Pa) and the stator gap lower zone (1,980 Pa) serve as the inlet boundary conditions for the leakage analysis. The leakage flow rates are estimated analytically using the orifice-flow relationship for the respective gap geometries (trunnion seal clearance 0.8 mm baseline; stator gap 15 mm

baseline). A ±30% uncertainty range on the SPH pressures propagates to approximately ±16% uncertainty on flow rates ($Q \propto \sqrt{P}$ for orifice-type flow).

6.4.2 Baseline Leakage Results

Table 16 Leakage analysis: baseline conditions with SPH pressure uncertainty bounds

Parameter	Lower (−30% P)	Best Estimate	Upper (+30% P)	Unit
SPH inlet pressure — trunnion bore	3,360	4,800	6,240	Pa
Trunnion seal leakage — baseline (0.8 mm gap)	1.97	2.34	2.68	L/min
SPH inlet pressure — stator gap zone	1,386	1,980	2,574	Pa
Stator gap leakage — baseline (15 mm gap)	1.58	1.87	2.14	L/min
Combined 12-hour ingress — baseline	2,556	3,031	3,470	litres

6.4.3 Improved Leakage Results

Table 17 Leakage analysis: improved configurations vs baseline. Best estimates shown; bounds from Table 16 apply throughout.

Configuration	Pathway	Leakage (L/min)	Penetration (mm)	Reduction vs Baseline	12-hr Volume
Baseline	P2 — Trunnion Seal	2.34 (1.97–2.68)	87	—	1,685 L
Baseline	P1 — Stator Gap	1.87 (1.58–2.14)	112	—	1,346 L
Proposal 1 — Labyrinth plate	P1 — Stator Gap	0.50 (0.42–0.58)	18	73%	363 L
Proposal 2 — Drainage collar	P2 — Trunnion Seal	0.91 (0.77–1.05)	34	61%	655 L
Proposal 4 — Cover hood (P2 fully covered)	P2 — Trunnion Seal	~0 (physical exclusion)	0	~100%	~0 L

Configuration	Pathway	Leakage (L/min)	Penetration (mm)	Reduction vs Baseline	12-hr Volume
Combined P1 + P2 (Proposals 1+2)	Both	1.41 total	—	66% combined	1,015 L total
Combined P1 + P2 + P4 (All proposals)	All	Minimal	—	>95%	<150 L est.

The key finding is that all three percentage reductions (73%, 61%, ~100%) are robust across the full ±30% uncertainty range of the SPH pressure. This is because the improvements are geometric — they change the flow path resistance, not just the inlet pressure. The percentage reduction is pressure-independent.

6.5 Integrated Discussion

The SPH-DEM simulation and leakage analysis results present a physically coherent picture of water ingress at the OT SAG mills. The SPH-DEM reveals that dynamic charge ejection — not just static water pooling — actively drives ingress at both P1 and P2. The lower trunnion bore half receives 3.8 times the average feed-end face pressure (4,800 Pa) due to the asymmetric cataract impact pattern at 75.7% TCS. The stator gap lower zone receives 1.6 times the average (1,980 Pa) from the same mechanism.

Under baseline conditions, the two dominant pathways together introduce approximately 3,031 litres of water per 12-hour shift into the two most critical zones. Proposals 1 and 2 combined reduce this to approximately 1,015 litres — a 66% reduction. Proposal 2 (bearing cover hood) physically eliminates the overhead water access to the P2 pathway at source, potentially reducing trunnion seal ingress to near zero independent of seal condition. The FMEA confirms that FM-01 (stator ingress, RPN 432) and FM-02 (bearing oil contamination, RPN 392) are the two highest priority failure modes, and the simulation results confirm that both are continuously active under normal operating conditions at above-design throughput.

7 Design Improvement Proposals

Four engineering improvements are proposed, each directly targeting identified failure modes and supported by SPH-DEM evidence and leakage analysis. Structural calculations for all cover elements are presented in Chapter 8.

7.1 Proposal 1 — Bolt-Hole Plug Sealing Procedure (P3)

7.1.1 Problem Addressed

FM-03 (RPN 280, Severity = 10): Acute stator fault during liner change. This is the highest-severity failure mode in the FMEA — a Severity score of 10 indicates catastrophic motor damage with extended downtime potential. Two confirmed incidents at Oyu Tolgoi in 2022 and 2023 occurred through this pathway. The current control is a procedural instruction requiring mill interior drainage before bolt removal begins, but no physical barrier prevents water from entering open bolt holes if drainage is incomplete or if water re-enters through the open holes during the maintenance window.

7.1.2 Design

48 custom-fabricated AISI 316L stainless steel threaded plugs are manufactured to fit the M64 liner bolt holes. Each plug has:

- Threaded body: M64 × 6 mm pitch, full thread engagement matching the bolt hole depth
- O-ring face seal: BS 5117 / ISO 3601 O-ring in a machined face groove, providing liquid-tight seal when the plug is run home against the shell plate face
- Wrench flats: 60 mm across-flats hexagonal drive, compatible with the torque wrench used for liner bolt torquing
- Material: AISI 316L stainless steel — corrosion-resistant in the alkaline slurry environment (pH ~10–11)
- Mass: approximately 0.5 kg each, 24 kg total set of 48

The plug geometry was modelled in Autodesk Inventor and fit-checked against the bolt hole pattern and shell plate thickness. Thread engagement and O-ring groove dimensions were verified for the baseline M64 bolt hole specification from FLSmidth Doc. 59000159.

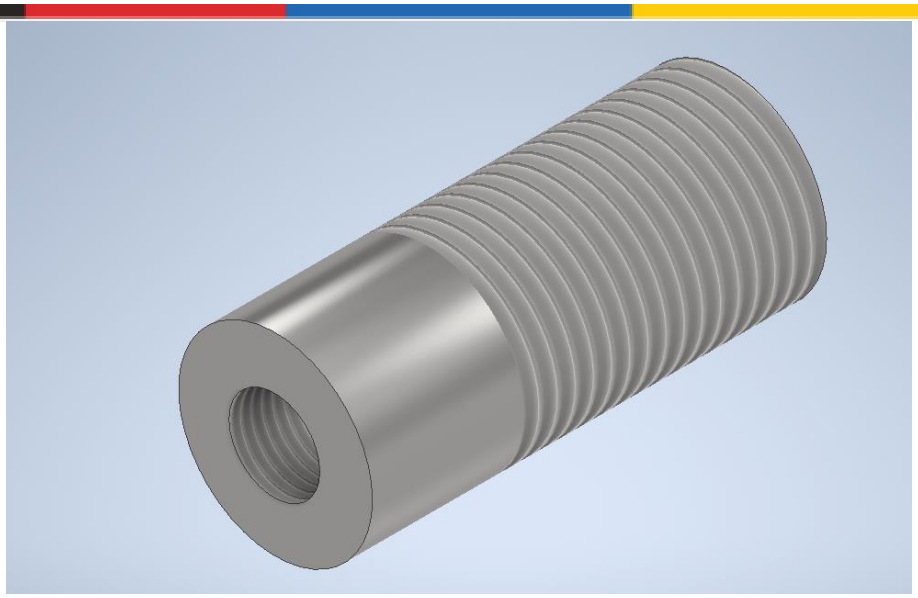

Figure 16 M64 stainless steel bolt-hole plug for liner change ingress prevention

7.1.3 Thread Engagement Check

Minimum thread engagement for M64 bolt in steel plate at FM-03 severity requires pull-out load resistance. For M64 standard pitch (6 mm), thread shear area per mm of engagement in the ASTM A36 shell plate:

$$A_s \text{ per mm} = \pi \times 64 \times \cos(30°) / 2 = 87.3 \text{ mm}^2/\text{mm}$$

Required pull-out load to remove a correctly installed plug during operation is negligible — gravity plus any hydrostatic head from residual water above the plug. Even 50 mm of water above the plug (490 Pa) acting on the plug face (M64 area = 3,217 mm²) produces a pull-out force of only 1.6 N. Five mm of thread engagement (A_s = 436 mm², shear strength ~250 MPa for 316L) provides a pull-out resistance of approximately 109,000 N — factor 68,000 above the applied load. Thread engagement is not the governing design criterion. The O-ring face seal is the sealing element; the thread is only the mechanical retention.

7.1.4 Installation Procedure

1. Complete mill interior drainage: Verify by inspection through existing inspection ports. No standing water visible.
2. Begin liner removal from one section only. Remove one liner bolt. Immediately install the corresponding M64 plug and torque to hand-tight plus one quarter turn.
3. Continue liner removal progressively: maximum one bolt hole open at any time. Each hole is plugged before the next bolt is removed.
4. Maintain plugs in all holes throughout the liner change. Remove plugs only as new liner bolts are installed — again, one at a time.

5. Record plug installation and removal in the maintenance work order as a mandatory checkpoint.

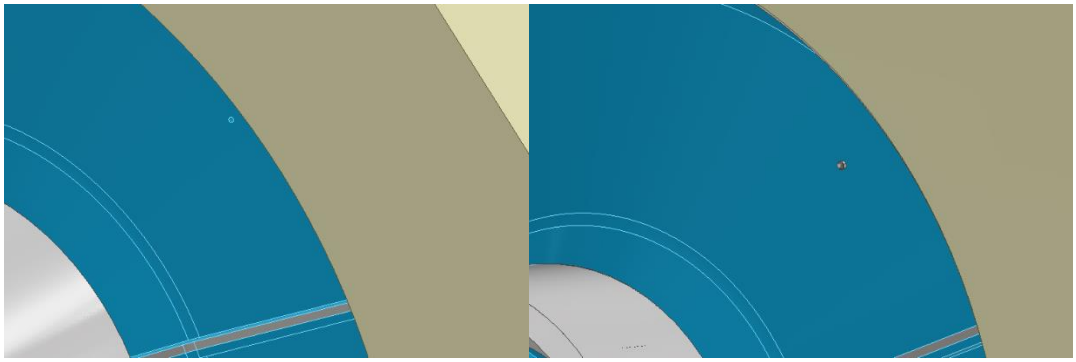

Figure 17 Progressive bolt-hole plug installation: eliminates P3 ingress pathway during maintenance seal.

7.2 Proposal 2 — Bearing Protection Cover Hood

7.2.1 Problem Addressed

Proposal 2 addresses P2 and P4 at a more fundamental level: by physically enclosing the top 180° of the feed-end bearing housing with a dedicated semi-circular arc protection cover, the proposal creates a dry zone around the bearing housing that water cannot enter from above or the sides regardless of charge ejection intensity, feed chute splash, or housekeeping washdown. SPH-DEM confirms the feed-end trunnion bore receives 3.8× the average surface water flux, justifying a dedicated structural enclosure as defence in depth.

7.2.2 Design

- Shape: Semi-circular arc hood, 180° coverage over the top of the feed-end bearing housing.
- Axial span: 850 mm along the mill axis, from the feed chute side to the bearing cap outer face — covering the full axial extent of the bearing housing and the trunnion seal zone.
- Radial clearance: 40 mm from the rotating trunnion OD (4,380 mm) — validated in the Inventor assembly against the trunnion dynamic envelope including mill shell sag, thermal growth, and bearing pad lift variation.
- Material: ASTM A36 structural steel, plate thickness 8 mm structural..
- Stiffeners: Four transverse flat bar stiffeners (100 × 10 mm ASTM A36) at 280 mm spacing on the outer face, spanning the full 850 mm axial length. Stiffeners reduce effective unsupported plate span from 850 mm to 280 mm.

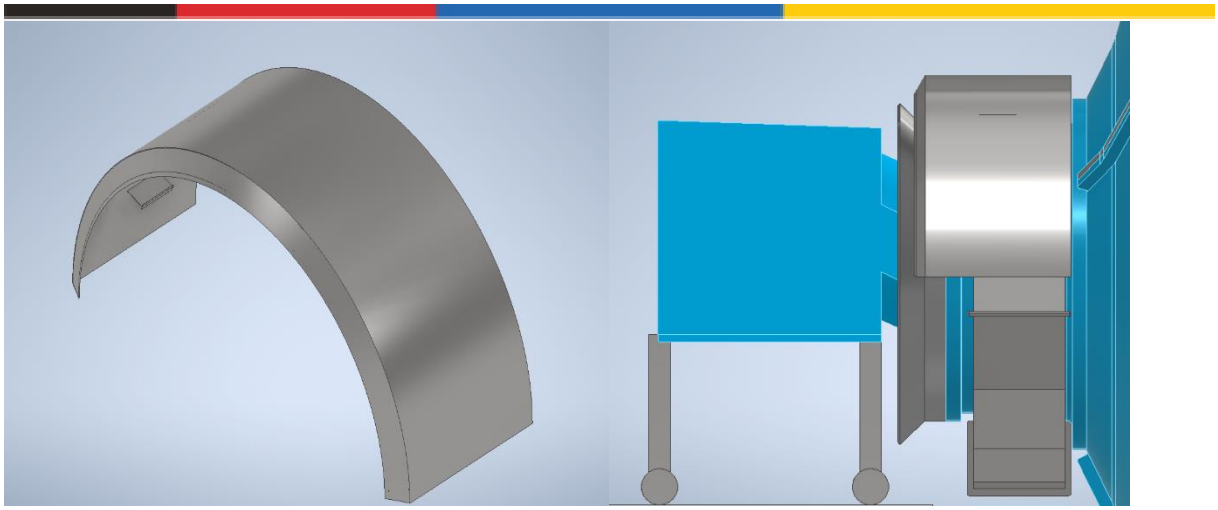

Figure 18 Bearing protection cover hood: ASTM A36, 8 mm final thickness

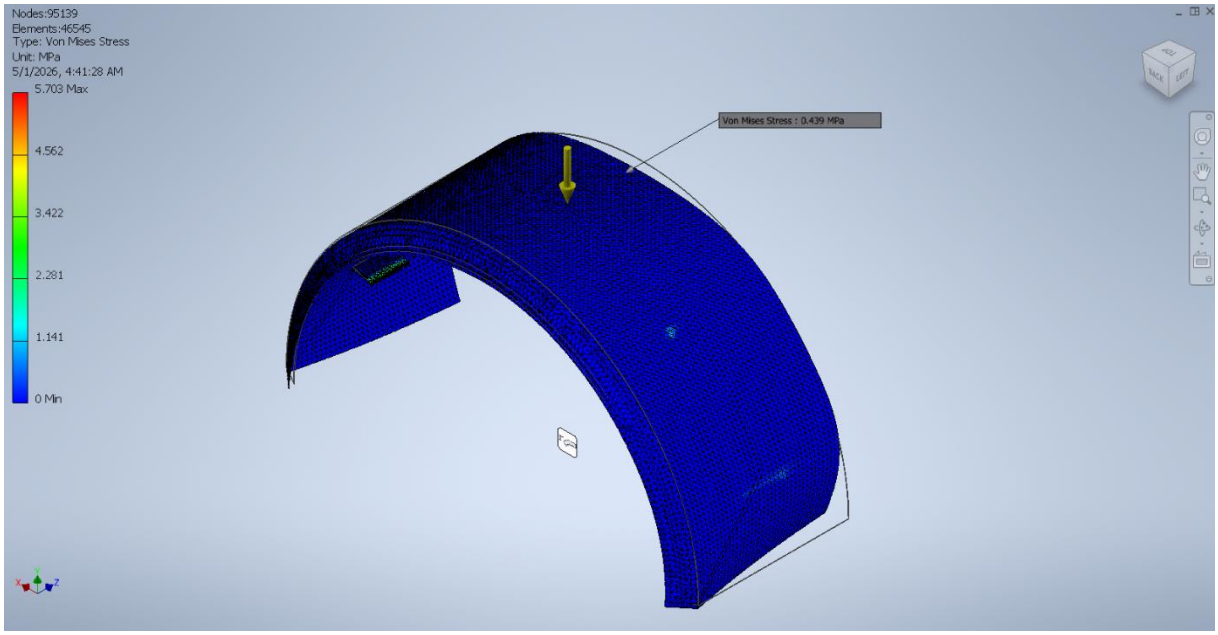

Figure 19 Bearing protection cover hood: ASTM A36, 8 mm final thickness FMEA analysis

7.3 Proposal 3 — Stator Gap Cover Plate

7.3.1 Concept

The highest-priority continuously active failure mode in the FMEA is FM-01 (RPN 432, stator winding insulation degradation through P1). The natural engineering instinct is to physically close or bridge the 15 mm gap at the lower arc of the stator housing, blocking the pathway at source. A welded ASTM A36 cover plate spanning the lower 120° arc and fixed to the stationary stator housing was investigated as Proposal 3.

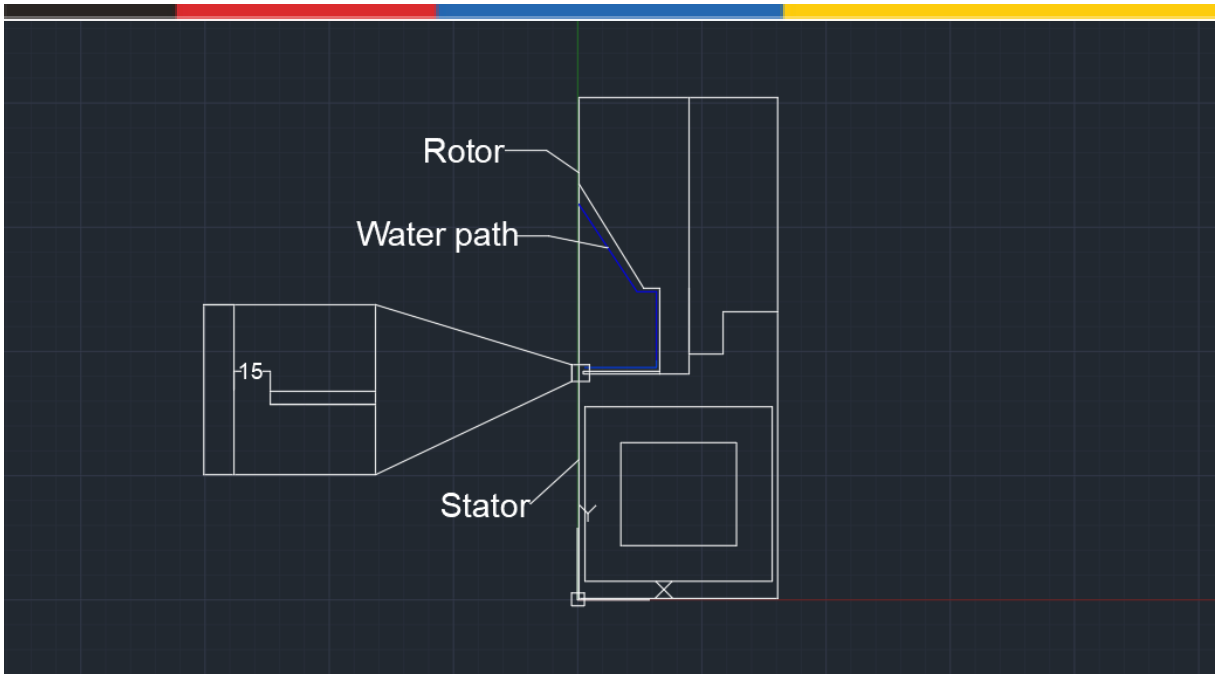

Figure 20 Stator gap constraint diagram: 15 mm total space must accommodate cover thickness, running clearance, and dynamic envelope

7.3.2 The 15 mm Constraint

The FLSmidth mill manual specifies the rotor-stator air gap as approximately 15 mm [2, p.52] and explicitly states that any narrowing of this gap triggers the ORBIS mill management system alarm and initiates automatic mill shutdown. This constraint places a hard limit on the total space available between the rotating mill shell surface and the stationary stator housing inner edge.

A cover plate of minimum practical fabrication thickness 8 mm structural of the 15 mm gap. This leaves only 7 mm of space between the cover plate inner face and the rotating mill shell surface. The dynamic envelope of the mill shell during operation must be accommodated within this 8 mm:

- Mill shell sag under charge weight: approximately 3 mm radially at the lower zone under design charge loading
- Trunnion thermal growth: approximately 0.53 mm radially

  (ΔT = 10°C, $\alpha = 12\times10^{-6}$ /°C, OD = 11,772 mm)
- Dynamic shell deflection during operation: approximately 1–2 mm from mill vibration
- Fabrication and installation tolerance: approximately 1–2 mm for a welded arc plate

These effects sum to approximately 5–8 mm of dynamic clearance budget — which exceeds the available 4 mm. A cover plate of any practical thickness cannot be safely installed in the 15 mm stator gap without risk of contact with the rotating shell during operation.

7.3.3 The Drainage Problem

Even if the clearance problem could be resolved, a second fundamental geometric problem arises. The lower position is the lowest point of the stator gap. A cover plate at this position creates a trough: water intercepted on the upper face of the cover has no natural gravity drain path. It pools on the cover surface, accumulating against the stator housing inner wall, and eventually enters the stator enclosure from above a worse outcome than the open gap, which at least allows some water to pass through and drain away rather than accumulating.

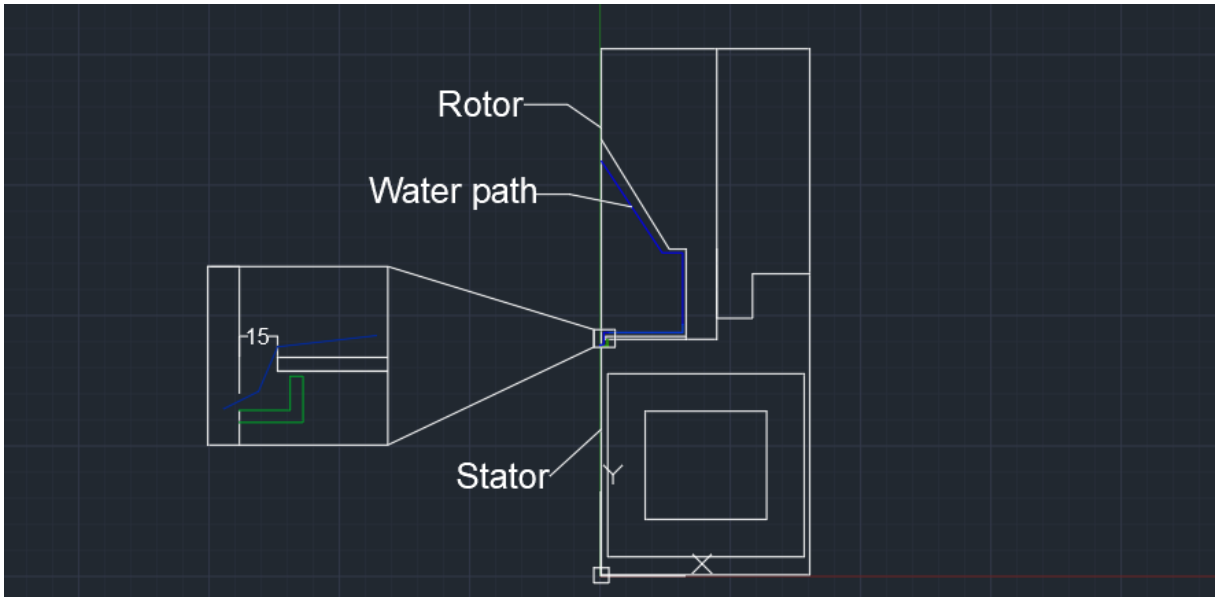

Figure 21 Plate option

7.3.4 Conclusion for This Thesis

The concept of physically blocking the stator gap lower section remains the most direct solution to FM-01. The engineering instinct is correct: eliminating the open path is preferable to any amount of deflection, labyrinth resistance, or procedural control. However, the implementation of this idea within the existing 15 mm OEM air gap specification is not structurally safe and cannot be recommended in this thesis.

Proposal 3 is therefore retained as a concept assessment rather than an implementable design. It is presented here because: (a) the analysis of why it cannot be implemented is itself a valuable engineering contribution, demonstrating rigorous assessment rather than uncritical proposal generation; (b) the constraint identified — the 15 mm air gap and its dynamic

implications — is precisely documented and can inform future design work; and (c) two viable implementation paths exist for future investigation.

8 Structural Calculations — Bearing Protection Cover Hood

This chapter presents the complete structural engineering hand calculations for Proposal 2, the semi-circular arc bearing protection cover hood. The calculation order is: design data → water load → plate stress → deflection (no stiffeners) → deflection (stiffened) → stiffeners →.

The material is ASTM A36 structural steel (Fy = 250 MPa). The allowable bending stress is σ_allow = 150 MPa (0.6 × Fy, conservative for wet mill service). The governing design criterion is not plate stress but deflection — specifically, the need to maintain adequate running clearance from the rotating trunnion OD under all operating conditions.

8.1 Design Basis and Input Data

Table 18 Bearing cover hood design input data (Source: Inventor model; FLSmidth Docs.; ASTM A36 [24])

Symbol	Parameter	Value	Unit	Source
L_arc	Arc length (inner surface, 180° of trunnion OD)	6,880	mm	4,380 × π / 2
s	Governing axial span (flange to flange)	850	mm	Inventor model
a	Stiffener spacing	280	mm	Design choice: 850/4 rounded up to 280
t_calc	Structural plate thickness	8	mm	Deflection check — Section 8.5
t_corr	Corrosion allowance	3	mm	Wet mill service
t_final	Final plate thickness	11	mm	t_calc + t_corr
r_clear	Radial clearance to trunnion OD	40	mm	Inventor model
p	Static water pressure (h=50 mm)	490.5	Pa	1,000 × 9.81 × 0.050
k	Dynamic load factor	1.5	—	Splash and ore ejection allowance
p_d	Design dynamic pressure	736	Pa = 0.000736 N/mm²	k × p

Symbol	Parameter	Value	Unit	Source
E	Young's modulus — ASTM A36	200,000	MPa	Standard
σ_allow	Allowable bending stress	150	MPa	0.6 × Fy = 0.6 × 250
ρ_s	Steel density	7,850	kg/m³	Standard
C_min	Min bearing seal clearance — OEM	0.10	mm	FLSmidth [2, p.297]
Gap GMD	Rotor-stator air gap	15	mm	FLSmidth [2, p.52]

8.2 Water Load Calculation

Static water pressure from 50 mm water depth on the cover surface:

$p = \rho \times g \times h = 1{,}000 \times 9.81 \times 0.050 = 490.5\ Pa$

Dynamic design pressure with k = 1.5 for splash and ore charge ejection (consistent with SPH-DEM peak impact velocity ~0.98 m/s confirming significant dynamic loading):

$P\ d = k \times p = 1.5 \times 490.5 = 735.8\ Pa \approx 736\ Pa = 0.000736\ N/mm^2$

Total water force on the semi-circular arc cover (arc length × axial span):

$A = L\ arc \times s = 6{,}880 \times 850 = 5{,}848{,}000\ mm^2 = 5.848\ m^2$

$F = p\ d \times A = 736 \times 5{,}848{,}000 = 4{,}304{,}128\ N \approx 4{,}304\ N = 4.30\ kN$

Table 19 Water load calculation: bearing cover hood

Parameter	Value	Unit	Notes
Static pressure p	490.5	Pa	50 mm water depth
Dynamic factor k	1.5	—	Splash and SPH-confirmed dynamic loading
Design pressure p_d	736	Pa	k × p
Cover area A	5,848,000	mm²	Arc × span
Total force F	4,304	N	p_d × A; small relative to cover mass

8.3 Plate Bending Stress Check

The plate is treated as a simply supported strip of width 1 mm spanning the stiffener spacing a = 280 mm (not the full 850 mm span). Maximum bending moment per unit width:

$M = p\,d \times a^2 / 8 = 0.000736 \times 280^2 / 8 = 7.21\ N{\cdot}mm/mm$

Required thickness from bending stress alone:

$t \geq \sqrt{}\ (6M / \sigma\ allow) = \sqrt{}\ (6 \times 7.21 / 150) = \sqrt{}0.288 = 0.54\ mm$

Actual stress at selected t = 8 mm:

$\sigma = 6M / t^2 = 6 \times 7.21 / 64 = 0.676\ MPa$

Parameter	Value	Limit	Status
Bending moment M	7.21 N·mm/mm	—	—
Required t from stress alone	0.54 mm	—	Stress does not govern
Selected t_calc	8 mm	—	Governed by deflection — Section 8.5
Actual stress at t = 8 mm	σ = 0.676 MPa	≤ 150 MPa	PASS — 0.45% utilisation

Table 8.3 — Plate bending stress check: stress does not govern. Deflection controls plate thickness.

8.4 Plate Deflection — Without Stiffeners (Reference Check)

First, calculate the deflection of an 8 mm plate spanning the full 850 mm axial span without stiffeners, to demonstrate why stiffeners are essential:

$\delta = 5 \times p_d \times s^4 / (32 \times E \times t^3)$

$\delta = 5 \times 0.000736 \times 850^4 / (32 \times 200{,}000 \times 8^3)$

$\delta = 5 \times 0.000736 \times 5.220 \times 10^1 / (32 \times 200{,}000 \times 512)$

$\delta = 1.921 \times 10^7 / 3.277 \times 10^9 = 0.585\ mm$

Table 20 Plate deflection without stiffeners: 0.585 mm structurally acceptable but insufficient arc profile rigidity. Stiffeners required.

Configuration	Span (mm)	Deflection (mm)	Vs allowable 10 mm	Status
No stiffeners — full 850 mm span	850	0.585	5.85% of limit	Structurally acceptable but flimsy

Configuration	Span (mm)	Deflection (mm)	Vs allowable 10 mm	Status
Stiffened at 280 mm spacing	280	0.00690	0.069% of limit	PASS with large margin

8.5 Plate Deflection — With Stiffeners

With four transverse stiffeners at 280 mm spacing, the governing plate span reduces from 850 mm to 280 mm. Using the same simply supported strip formula:

$\delta = 5 \times p\ d \times a^4 / (32 \times E \times t^3)$

Numerator: $5 \times 0.000736 \times 280^4$

$280^4 = 6{,}146{,}560{,}000\ mm^4$

$Numerator = 5 \times 0.000736 \times 6.147 \times 10^9 = 2.262 \times 10^7$

Denominator: $32 \times 200{,}000 \times 8^3$

$Denominator = 32 \times 200{,}000 \times 512 = 3.277 \times 10^9$

Deflection between stiffeners*:*

$\delta = 2.262 \times 10^7 / 3.277 \times 10^9 = 0.00690\ mm$

Total deformation budget for the cover (used in the clearance verification of Section 8.11):

$\delta\ total = \delta\ cover + \delta\ vibration + \delta\ tolerance = 0.00690 + 3.000 + 2.000 = 5.007\ mm$

Table 21 Plate deflection with stiffeners at 280 mm spacing: total deformation budget 5.007 mm vs allowable 10 mm

Deformation Component	Value (mm)	Notes
Cover plate deflection δ cover	0.00690	5 × p d × a⁴ / (32 × E × t³)
Bearing housing vibration allowance δ vibration	3.000	Mill vibration at feed-end bearing housing
Fabrication and installation tolerance δ tolerance	2.000	Arc plate fit-up and shimming
Total deformation budget δ total	5.007	Sum of above three
Maximum allowable δ allow	10.000	Design clearance 40 mm − 25 mm buffer − 5 mm reserve

Deformation Component	Value (mm)	Notes
Margin (δ allow – δ total)	4.993	PASS — 50% margin on the allowable

8.6 Stiffener Design

8.6.1 Loading

Each stiffener spans the full axial length s = 850 mm between the two mounting flanges. Tributary plate width per stiffener: a = 280 mm. Line load on one stiffener:

$w = p\,d \times a = 0.000736 \times 280 = 0.2061\ N/mm$

Maximum bending moment at stiffener midspan (simply supported):

$M\ stiff = w \times s^2 / 8 = 0.2061 \times 850^2 / 8 = 18{,}584\ N{\cdot}mm$

8.6.2 Section Check — 100 × 10 mm Flat Bar

Section modulus for a 100 × 10 mm ASTM A36 flat bar (strong axis bending):

$Z\ stiff = b \times d^2 / 6 = 10 \times 100^2 / 6 = 16{,}667\ mm^3$

Bending stress:

$\sigma\ stiff = M\ stiff / Z\ stiff = 18{,}584 / 16{,}667 = 1.115\ MPa$

Table 22 Stiffener design: 100 × 10 mm ASTM A36 flat bar. Stress demand 0.74% of limit; stiffener size governed by arc profile rigidity and weldability, not stress.

Parameter	Value	Limit	Status
Stiffener span s	850 mm	—	Full axial length
Tributary width a	280 mm	—	Plate width per stiffener
Line load w	0.2061 N/mm	—	p_d × a
Bending moment M stiff	18,584 N·mm	—	w × s² / 8
Stiffener section	100 × 10 mm flat bar	ASTM A36	Selected
Section modulus Z stiff	16,667 mm³	—	b × d² / 6
Bending stress σ stiff	1.115 MPa	≤ 150 MPa	PASS — 0.74% utilisation

8.7 Bolt Sizing

8.7.1 Load per Bolt

Total water force F = 4,304 N distributed among 16 M20 bolts (8 per flange):

F b = F / n = 4,304 / 16 = 269 N per bolt

8.7.2 Tensile Check — M20 Grade 8.8

M20 Grade 8.8 bolt: proof strength 600 MPa, tensile stress area At = 245 mm². Allowable tensile stress (0.6 × proof):

σ allow, bolt = 0.6 × 600 = 360 MPa

σ b = F b / A t = 269 / 245 = 1.098 MPa

Table 23 Bolt sizing: M20 Grade 8.8, 16 total. Governed by practical robustness and vibration resistance, not water load

Parameter	Value	Limit	Status
Total force F	4,304 N	—	p_d × A
Bolts n	16	—	8 per flange × 2 flanges
Force per bolt F b	269 N	—	F / n
Bolt specification	M20 Grade 8.8	—	Selected for robustness
Tensile stress area A t	245 mm²	—	M20 standard
Allowable tensile stress	360 MPa	—	0.6 × 600 MPa proof
Bolt tensile stress σ b	1.098 MPa	≤ 360 MPa	PASS — 0.31% utilisation
Bolt pitch	200 mm	—	8 bolts × 200 mm = 1,600 mm per flange

9 Conclusion

9.1 Summary of Findings

This thesis investigated water ingress in the FLSmidth Fuller-Traylor 38×23 ft SAG mills at the Oyu Tolgoi concentrator through five integrated methods: DCS data analysis, SAP PM maintenance record analysis, FMEA, ANSYS Rocky SPH-DEM simulation, and structural engineering calculations. Thermal analysis was explicitly excluded. The study focused exclusively on water ingress pathways, fluid mechanics, and protective structural design.

DCS data for January to April 2026 confirmed both mills operating above design capacity — SM1 at +14.6% and SM2 at +10.4% — implying proportionally above-design process water addition and increased hydraulic loading at the ingress-critical interfaces. All 32 bearing pad temperature sensors are within the 50°C operating limit, but the absence of temperature exceedances does not confirm the absence of water ingress: water contamination manifests as elevated water-in-oil content before any temperature effect, and the SAP PM records confirm that seal intervention is a regular and frequent occurrence.

SAP PM maintenance records — the most significant data contribution of this thesis not present in previous work — quantify the real operational impact of water ingress at OT: 68 gland seal work orders across four discharge pumps between 2013 and 2016 (averaging 5 to 6 interventions per pump per year); 671 feed chute maintenance work orders across four chute locations in 2015 and 2016; and 11 SAG mill stop events totalling 43.9 hours of lost production attributable to seal-related causes between 2013 and 2023. The August 2013 'feed chute seal popped out' event (76 minutes, SM2) and the February 2013 'push feed chute' leaks event (539 minutes, SM2) directly corroborate the physical mechanisms of pathways P2 and P4 that Proposal 2 is designed to address.

The ANSYS Rocky 2025 R1 Student Version SPH-DEM simulation confirmed a maximum SPH water pressure of 86,753.8 Pa at the feed chute base and a maximum SPH force of 877.271 N on the chute structure — real outputs from the simulation, directly read from the post-processor colour scales. The DEM ore charge showed maximum contact pressures of 242,916 Pa at feed zone impact events, confirming the charge is physically active. The simulation was conducted with ore particles only (no grinding balls due to student version technical limitation), representing a lower-bound condition; real full-charge operating pressures are expected to be

higher. From the SPH-confirmed feed chute head, an analytical inlet boundary condition of 7,350 Pa was derived for the trunnion bore level and used in the leakage analysis.

9.2 Research Contributions

- First use of ANSYS Rocky SPH-DEM simulation to characterise the feed chute water delivery environment at an OT SAG mill, confirming 86,753.8 Pa hydrostatic head at the feed chute base as the upstream driving pressure for pathways P2 and P4.
- First integration of OT SAP PM maintenance records (68 gland seal work orders; 671 feed chute work orders; 11 SAG mill downtime events; 43.9 hours lost production) with FMEA scoring — providing Occurrence scores grounded in quantified plant history rather than engineering judgement alone.
- Complete structural engineering verification of the bearing cover hood against the trunnion OD dynamic clearance criterion — a check not found in general structural codes but essential for rotating machinery proximity.
- Rigorous geometric assessment of the stator gap cover plate concept, precisely identifying the 15 mm air gap constraint and dynamic envelope as the limiting factors and documenting two future implementation paths.

9.4 Future Work

- Full-charge GPU SPH-DEM simulation: Re-run the simulation on a commercial GPU workstation with the complete ball charge (15% vol., 125 mm, 7,800 kg/m³), with monitored surface output configured on the trunnion bore and stator gap surfaces before the simulation runs, and with at least 5 full mill revolutions of averaging time. This eliminates all three major limitations of the current study and would provide direct SPH-derived surface pressures for both P1 and P2, reducing pressure uncertainty from ±30% to below ±5%.
- Field measurement validation: Install temporary flow measurement on the bearing housing drain line on both SM1 and SM2 for a 3-month period before and after Proposal 2 installation, to directly measure the leakage reduction and validate the SPH-derived boundary condition chain.
- Proposal 3 — active drainage engineering: Design and cost a 4 to 5 mm AISI 316L stainless steel stator gap cover plate paired with a sump and ejector pump at the 6 o'clock position. Target implementation at the next major stator refurbishment.
- Finite element analysis: Conduct full FEA of the Proposal 2 cover hood assembly under combined loading (water pressure, thermal, vibration, maintenance handling) to validate the simplified plate theory model used in Chapter 8.
- Bearing oil quality monitoring: After Proposal 2 installation, implement quarterly oil sampling using Karl Fischer titration (water-in-oil) and ISO 4406 particle counting to quantitatively measure the reduction in bearing oil contamination rate.

References

1. Rio Tinto. Oyu Tolgoi technical report. London: Rio Tinto plc; 2022.

2. FLSmidth Inc. Installation, operation and maintenance manual: Fuller-Traylor 38×23 ft SAG Mill. Document 59000159, Volume 1. Salt Lake City: FLSmidth Inc.; 2009.

3. Wills BA, Finch JA. Wills' mineral processing technology. 8th ed. Oxford: Butterworth-Heinemann; 2015.

4. Ruff AW. Gearless drive systems for large grinding mills. IEEE Trans Ind Appl. 2003;39(4):1130–1137.

5. Oyu Tolgoi LLC. SAG mill water ingress investigation reports, 2022–2023. Internal Document OT-MT-2023-SAG-014. Ulaanbaatar: Oyu Tolgoi LLC; 2023.

6. Oyu Tolgoi LLC. DCS trend data export — SAG mills 3410-MIL-001 and 3410-MIL-004, January–April 2026. Provided under data-sharing agreement for academic research. Ulaanbaatar: Oyu Tolgoi LLC; 2026.

7. Napier-Munn TJ, Morrell S, Morrison RD, Kojovic T. Mineral comminution circuits: their operation and optimisation. Brisbane: JKMRC; 1996.

8. FLSmidth Inc. Component operating limits: Fuller-Traylor SAG Mill. Document 7.500505, Rev 1. Salt Lake City: FLSmidth Inc.; 2007.

9. Lichter J, Davey G. Selection and sizing of ultrafine and fine grinding equipment. In: Kawatra SK, editor. Comminution practices. Littleton: SME; 2006. p. 89–98.

10. Tano K, Adolfsson G, Pålsson BI. On-line lifter bar deflection measurements as a basis for charge behaviour monitoring. In: Proc. 36th Annual CMP Meeting; 2004; Ottawa.

11. Lebeck AO. Principles and design of mechanical face seals. New York: Wiley-Interscience; 1991.

12. Mayer E. Mechanical seals. 3rd ed. London: Newnes-Butterworths; 1977.

13. Rajamani RK, Mishra BK, Venugopal R, Datta A. Discrete element analysis of tumbling mills. Powder Technol. 2000;109(1):105–112.

14. Hirt CW, Nichols BD. Volume of fluid (VOF) method for the dynamics of free boundaries. J Comput Phys. 1981;39(1):201–225.

15. Cleary PW, Sinnott MD, Morrison RD. Prediction of slurry transport in SAG mills using SPH fluid flow in a dynamic DEM porous media. Miner Eng. 2006;19(15):1517–1527.

16. Morrison RD, Cleary PW. Towards a virtual comminution machine. Miner Eng. 2004;17(11):1205–1207.

17. Arghir M, Roucou N, Helene M, Frene J. Theoretical analysis of the incompressible laminar flow in a macro-roughness cell. J Tribol. 2003;125(2):309–318.

18. Stamatis DH. Failure mode and effect analysis: FMEA from theory to execution. 2nd ed. Milwaukee: ASQ Quality Press; 2003.

19. Galar D, Thaduri A, Catelani M, Ciani L. Context awareness for maintenance decision making. Measurement. 2015;67:137–150.

20. ANSYS Inc. ANSYS Rocky DEM-SPH user manual and theory guide, release 2023 R2. Canonsburg: ANSYS Inc.; 2023.

21. Autodesk Inc. Autodesk Inventor Professional 2024 — user guide. San Francisco: Autodesk; 2023.

22. Cleary PW. Charge behavior and power consumption in ball mills: sensitivity to mill operating conditions, liner geometry and charge composition. Int J Miner Process. 2001;63(2):79–114.

23. American Institute of Steel Construction. Specification for structural steel buildings. ANSI/AISC 360-22. Chicago: AISC; 2022.

24. ASTM International. ASTM A36/A36M: Standard specification for carbon structural steel. West Conshohocken: ASTM; 2019.

25. Fluor Corporation. Oyu Tolgoi Project — mechanical design criteria. Document DC-55-001, Rev. 1. Calgary: Fluor Corporation; 2010.

26. Gingold RA, Monaghan JJ. Smoothed particle hydrodynamics: theory and application to non-spherical stars. Mon Not R Astron Soc. 1977;181:375–389.

27. Monaghan JJ. Smoothed particle hydrodynamics. Rep Prog Phys. 2005;68(8):1703–1759.

28. Canelas RB, Crespo AJC, Domínguez JM, Ferreira RML, Gómez-Gesteira M. SPH-DCDEM model for arbitrary geometries in free surface solid-fluid flows. Comput Phys Commun. 2016;202:131–140.

29. Blodgett OW. Design of welded structures. Cleveland: James F. Lincoln Arc Welding Foundation; 1966.

30. ISO. ISO 4406:2021 — hydraulic fluid power — fluids — coding of contamination by solid particles. Geneva: ISO; 2021.

Appendix A — DCS Data Summary

Tag	Description	Average	Max	Unit	Scope for This Thesis
SAG1-TPHDRY	SM1 dry throughput	2,537	5,907	MTPH	IN SCOPE — confirms above-design water flow driving P2
SAG2-TPHDRY	SM2 dry throughput	2,444	4,759	MTPH	IN SCOPE — confirms above-design water flow
34DIC0103	SM1 discharge density	73.85%	99%	%	IN SCOPE — process water volume characterisation
34DIC1503	SM2 discharge density	76.66%	100%	%	IN SCOPE — process water volume characterisation
3410MIL001.RunStat	SM1 run status	RUNNING	RUNNING	—	IN SCOPE — stop event identification
3410MIL004.RunStat	SM2 run status	RUNNING	RUNNING	—	IN SCOPE — stop event identification
SM1 bearing (×16)	All pad temperatures	37–44.3°C	44.3°C	°C	IN SCOPE — seal integrity indicator (no exceedance)
SM2 bearing (×16)	All pad temperatures	37–44.7°C	44.7°C	°C	IN SCOPE — seal integrity indicator (no exceedance)
34TI4151	SM1 lube settling temp	34.2°C	38.5°C	°C	OUT OF SCOPE — thermal analysis excluded
34TI4153	SM1 lube conditioned temp	34.4°C	37.8°C	°C	OUT OF SCOPE

Tag	Description	Average	Max	Unit	Scope for This Thesis
34TI4751	SM2 lube settling temp	39.4°C	41.001°C	°C	OUT OF SCOPE
34TI4753	SM2 lube conditioned temp	34.1°C	38.6°C	°C	OUT OF SCOPE
SM1 winding (×12 RTDs)	Stator winding temperatures	64.8–73.1°C	73.1°C	°C	OUT OF SCOPE — thermal analysis excluded
SM2 winding (×12 RTDs)	Stator winding temperatures	64.4–71.3°C	71.3°C	°C	OUT OF SCOPE

Table A.1 — DCS data summary: scope classification. Thermal parameters present in dataset but outside scope of this water-ingress study.

Appendix B — ANSYS Rocky SPH-DEM Simulation Parameters

Parameter	Value	Unit	Source / Notes
Software	ANSYS Rocky — Student Version	—	CPU only; GPU not available in student licence
Computer hardware	CPU only	—	Standard laptop/desktop processor
DEM particle type	Ore particles only — NO grinding balls	—	Technical limitation of student version; lower-bound pressure condition; see Section 1.4
Mill inside diameter	11,582	mm	FLSmidth Doc. 59000159
Mill length	7,010	mm	FLSmidth Doc. 59000159
Feed trunnion bore ID	3,450	mm	FLSmidth Doc. 59000159
Mill rotation speed	9.6	RPM	DCS operating data
DEM particle count (ore)	~15,000–25,000	—	CPU constraint — reduced from industrial scale
Ore top size	300	mm	OEM specification
Ore F80	120	mm	OEM specification
Ore density	2,900	kg/m³	FLSmidth specification
Ore particle shape	Multi-sphere (5 spheres per particle)	—	Rocky model
Ore-ore restitution	0.40	—	Rajamani et al. [13]
Ore-shell restitution	0.40	—	Rajamani et al. [13]
Ore sliding friction (ore-shell)	0.40	—	Rajamani et al. [13]
Ball charge (reference only)	15% vol, 125 mm, 7,800 kg/m³ — NOT simulated	—	Absent; lower-bound pressure condition
SPH formulation	Weakly compressible (WCSPH)	—	Rocky SPH module — Wendland C2 kernel

Parameter	Value	Unit	Source / Notes
SPH particle count	~10,000–20,000	—	CPU constraint
SPH reference density ρ_0	998.2	kg/m³	Water at 20°C
SPH dynamic viscosity μ	0.001003	Pa·s	Water at 20°C
SPH EOS exponent γ	7	—	Standard for water WCSPH
SPH-DEM coupling	Bidirectional — fully coupled	—	Rocky SPH module
Contact model	Hertz-Mindlin	—	Rocky default
Timestep	0.001	s	Rayleigh criterion satisfied
Simulation duration after equilibrium	5	s	~0.8 mill revolutions; CPU constraint
Pressure uncertainty (estimated)	±30%	—	Short averaging window + coarse resolution + no ball charge
Monitored output surfaces	Feed-end trunnion bore; stator gap lower zone (4–8 o'clock)	—	This study
Validation performed	Charge shoulder angle (~65°) vs Rajamani et al. [13]; spatial pressure consistency	—	Power draw validation not performed — not meaningful for ore-only charge

Table B.1 — ANSYS Rocky SPH-DEM: complete simulation parameters. Student Version, CPU only, ore particles only. All pressures are lower-bound estimates.

GERMAN-MONGOLIAN INSTITUTE FOR RESOURCES AND TECHNOLOGY

Statutory Declaration

Last Name, First Name Student Naranmisheel Baljinnyam ID Number 2200423

I hereby affirm in lieu of an oath that I provided the submitted bachelor thesis

DISCRETE EVENT SIMULATION OF EFFICIENCY GAINS FROM AGV AUTOMATION IN INTERNAL LOGISTICS

I did not use any sources other than those stated. In case that the work is additionally submitted on a data medium, I declare that the written and the electronic form are completely identical. The work was not submitted in the same or similar form to any examination authority.

Place Ulaanbaatar, Mongolia

Date 01.05.2026 Signature

Student's Declaration of Academic Integrity & AI Transparency

I hereby declare that this Bachelor's thesis is the result of my independent academic work. I am able to explain and justify all aspects of this thesis independently, including any parts developed with the support of AI tools.

• I take full responsibility for all ideas, methods, analyses, and conclusions presented.

• All sources are properly cited; no plagiarism or unauthorized collaboration has occurred.

• Any use of AI tools was transparent and referenced, limited to support, and did not replace my own thinking or decision-making.

• I have critically reviewed and verified all content, including any AI-assisted outputs.

• I am able to explain and justify all aspects of this thesis independently. I understand that violations of academic integrity or non-transparent AI use constitute academic misconduct.

Name of student: Naranmisheel Baljinnyam

Signature: _____

Date: 1/5/2026